Modeling growth of cultured neocortical neuronal networks: Comparison of the simulation tools CX3D and NETMORPH

Master's Thesis
Riikka Havela
Institute of Biomedical Technology
University of Tampere
May 2011

Preface

This M.Sc. thesis was completed in the Laboratory of Computational Neuroscience (CNSL) at Tampere University of Technology (TUT), Finland.

First, I wish to express my sincere gratitude to my thesis supervisors Adjunct Professor Marja-Leena Linne, Ph.D., and Senior Researcher Jugoslava Aćimović, Ph.D., for guiding me to the fascinating research area of computational neuroscience, and giving me a wealth of valuable advice, support and inspiration. I also express my warmest thanks to Tiina Manninen, Ph.D., Tuomo Mäki-Marttunen, M.Sc., Heidi Teppola, M.Sc., Jukka Intosalmi, M.Sc., Katri Holm, M.Sc. and Eeva Toivari, M.Sc., for the wonderful work atmosphere and help they have given me during my time in CNSL.

Finally, I want to thank Jouni, who has provided me with much appreciated delicious meals during my M.Sc. work, as well as my family, for supporting me at all times.

Tampere, May 2011

Riikka Havela

MASTER'S THESIS

Place:	UNIVERSITY OF TAMPERE Institute of Biomedical Technology
Author:	HAVELA, RIIKKA CHARLOTTA
Title:	Modeling growth of cultured neocortical neuronal networks: comparison of the simulation tools CX3D and NETMORPH
Pages:	77 pp.
Supervisors:	Senior Researcher, Adjunct Professor Marja-Leena Linne, Ph.D.; Senior Researcher Jugoslava Aćimović, Ph.D.
Reviewers:	Professor Markku Kulomaa; Senior Researcher, Adjunct Professor Marja-Leena Linne, Ph.D.
Time:	May 2011

ABSTRACT

Background and aims: Development of neuronal morphology and formation of networks is an elaborate process determining the information processing capabilities of the formed network. The early phases of this process are readily studied *in vitro*, but are so far incompletely understood. Computational modeling can help in revealing the mechanisms of development of neuronal networks. The aim of this work was to compare two recently published simulators of neuronal growth, CX3D and NETMORPH, by implementing in them a model of growth of neurons in culture.
Methods: Three different models were built and simulated with parameter values determined based on the literature. The first model has 100 interconnected neurons and was simulated on both CX3D and NETMORPH varying the neurite growth rate parameters. The second model has 1000 neurons and was simulated with NETMORPH. The third model has 100 neurons and was simulated with CX3D varying the attraction parameter. Sholl analysis was used to analyze the produced single neuron morphologies, and graph theoretical measures (in-degree, shortest path length, motifs) were used to quantify features of the simulated neuronal networks.
Results: Based on the quantification of numbers of synapses, CX3D simulations produced neuronal networks closest to the experimentally observed ones, but Sholl analysis revealed in some cases unrealistic features in morphologies of neurites. Also, the simulations were computationally heavy. NETMORPH also produced realistic results, but with excessive numbers of synapses per neuron. The simulations, however, were lighter. Proportional to the number of synapses, the graph theoretical measures behaved similarly with both simulation tools.
Conclusions: Implementing the same model in both CX3D and NETMORPH is not straightforward. Thus, they also produced differing results with the same set of simulated parameters. However, with a correct choice of parameters, both simulation tools are capable of producing qualitatively similar results. Both tools produce results that are in the range of experimentally observed values. The different nature of the tools suggest different applications. CX3D would be suited for models that have molecular guidance cue diffusion, and NETMORPH for graph theoretical studies of large neuronal networks.

PRO GRADU -TUTKIELMA

Paikka:	TAMPEREEN YLIOPISTO Biolääketieteellisen teknologian yksikkö
Tekijä:	HAVELA, RIIKKA CHARLOTTA
Otsikko:	Viljeltyjen neokorteksin hermosoluverkkojen kasvun mallintaminen: CX3D– ja NETMORPH–simulaatiotyökalujen vertailu
Sivumäärä:	77 s.
Ohjaajat:	Vanhempi tutkija, dosentti, TkT Marja-Leena Linne; Vanhempi tutkija, FT Jugoslava Aćimović
Tarkastajat:	Professori Markku Kulomaa; Vanhempi tutkija, dosentti, TkT Marja-Leena Linne
Aika:	Toukokuu 2011

TIIVISTELMÄ

Tutkimuksen tausta ja tavoitteet: Hermosolujen morfologian ja hermoverkkojen muodostuminen on prosessi, joka määrittää muodostuneen verkon tiedonkäsittelykyvyn. Prosessin varhaisia vaiheita on mahdollista tutkia *in vitro*, mutta niitä ymmärretään edelleen huonosti. Laskennalliset mallit voivat auttaa ymmärtämään hermoverkkojen kehityksen mekanismeja. Tämän työn tavoitteena oli vertailla kahta uutta hermoverkkojen kasvua simuloivaa työkalua, CX3D:tä ja NETMORPH:ia, implementoimalla molempiin hermosolujen kasvua viljelmissä kuvaavan mallin.
Tutkimusmenetelmät: Kolme mallia rakennettiin ja niitä simuloitiin kirjallisuuden perusteella valituilla parametrien arvoilla. Ensimmäinen malli, jossa on 100 hermosolua, simuloitiin sekä CX3D:llä että NETMORPH:illa vaihdellen neuriittien kasvunopeuden parametrien arvoja. Toista mallia simuloitiin vain NETMORPH:illa. Toisessa mallissa on 1000 hermosolua. Kolmannessa mallissa on 100 hermosolua, ja sitä simuloitiin CX3D:llä vaihdellen houkutusparametrin arvoja. Hermosolujen morfologiaa analysoitiin Sholl-analyysilla, ja hermosoluverkkojen piirteitä (tuloaste, lyhin polku ja motiivit) graafiteorian menetelmin.
Tutkimustulokset: Synapsien määrän perusteella arvioituna CX3D-simulaatiot tuottivat kokeellisesti havaittuja hermosoluverkkoja lähimpänä olevia tuloksia, mutta Sholl-analyysi paljasti epärealistisia morfologioita hermosoluilla. Simulaatiot olivat myös laskennallisesti raskaita. NETMORPH tuotti samankaltaisia tuloksia kuin CX3D, mutta synapsien määrä hermosolua kohti oli liian suuri. Simulaatiot olivat kuitenkin kevyempiä. Synapsien määrään suhteutettuna graafiteorian analyysimenetelmät tuottivat samanlaisia tuloksia molemmilla työkaluilla simuloiduille verkoille.
Johtopäätökset: Johtuen CX3D:n ja NETMORPH:in erilaisista ominaisuuksista, mallin täsmälleen yhtäläinen implementointi ei ole mahdollista. Siksi ne tuottivat erilaisia simulaatiotuloksia samoilla parametreilla. Valitsemalla parametrit oikein molemmat voidaan kuitenkin saada tuottamaan laadullisesti samankaltaisia tuloksia. Kumpikin työkalu tuottaa biologisissa kokeissa havaittujen kaltaisia tuloksia. Koska nämä työkalut ovat luonteeltaan erilaisia, niille sopivat erilaiset käyttötarkoitukset. CX3D sopii parhaiten malleille joissa on mukana houkutusmolekyylien diffuusiota, ja NETMORPH taas suurten verkkojen graafiteoreettiseen tarkasteluun.

Contents

Abbreviations

ACh	Acetylcholine
Ara-C	Cytosine arabinoside
CNS	Central nervous system
DIV	Day(s) *in vitro*
DMEM	Dulbecco's Modified Eagle's Medium
GABA	γ-aminobutyric acid
MEA	Microelectrode array
NgCAM	Neuron-glia cell adhesion molecule
PDL	Poly-D-lysine
PEI	Polyethyleneimine
PL	Polylysine
PLL	Poly-L-lysine
W.R.T	With respect to

1 Introduction

Deciphering of neuronal functions started in the late 19^{th} century by recognition of different types of neuronal processes, axons and dendrites. The general mechanisms of propagation of bioelectrical signals between neurons was largely discovered in the mid-20^{th} century. However, increasing knowledge has led to understanding that neuronal signal propagation is far more complicated than originally thought (see *e.g.* Manninen et al., 2010). Physical, chemical and morphological properties of neurons and their environment affect the processing and propagation of signals in ways not yet properly understood.

In the neuronal connectivity scheme, the morphology of axons and especially denrites is a key factor (Stepanyants & Chklovskii, 2005). Dendrites form an elaborate tree-like structure which is characteristic of each neuronal cell type. Morphology of the dendritic tree determines the extent of connectivity to other neurons a neuron can have (Purves et al., 2008). The scientific knowledge about the mechanisms and dynamics of dendritic tree development is still far from complete.

Data from experiments and computer simulations indicates that morphology of the dendritic tree also has a profound effect on action potential firing properties of neurons (Segev, 2006; Bekkers & Häusser, 2007; van Elburg & van Ooyen, 2010). Mechanisms of morphological development of dendritic and axonal structures are hence a central topic in understanding the development of functions of neurons in neuronal networks, which form the basis of neuronal signal propagation and processing.

This M.Sc. thesis attempts to contribute to the study of developing neuronal networks. In this thesis, two novel tools for simulating the growth of neurons and generation of neuronal networks, CX3D (Zubler & Douglas, 2009) and NETMORPH (Koene et al., 2009b), are tested and evaluated. This work focuses solely on simulating the growth of dissociated neocortical cell cultures. The choice is due to the simplified and easily observable experimental setting they represent, and because they readily enable application of new data about neuronal growth into new experimental designs.

The results presented here have, in part, been published in Workshop for Computational Systems Biology 2010 in Luxembourg (Mäki-Marttunen et al., 2010), and in EURASIP Journal on Bioinformatics and Systems Biology (Aćimović et al., 2011).

2 Review of the literature

2.1 Features of neocortical cell biology

2.1.1 Principles of single neuron development

The formation of the central nervous system (CNS) starts early on during the embryonic development, when neural ectoderm is generated from the ectodermal cell layer of the embryo. The differentiation of neuronal stem cells into different cell types of the brain starts after the developing of the neural tube into a primitive brain and spinal cord has finished. Stem cells located in the ventricular zone divide to produce transit amplifying cells. These cells are distinct from the stem cells in that they divide very rapidly, and are committed to further differentiation into neuroblasts which give rise to neurons and glial cells. Different cell populations of the spinal cord and nuclei in the brain are generated at distinct times during the neuroblast generation. Neurogenesis takes place first, followed by oligedendrogenesis and astrogliogenesis, in that order (Purves et al., 2008).

When neurons and glia have migrated to their final destinations in the developing CNS, the neural circuit formation starts. For this purpose, neurons start to grow axons, which later transmit action potentials to other neurons, and dendrites, which can receive the signals from other neurons' axons. Together, axons and dendrites are called neurites. The tip of a growing neurite is a highly dynamic structure called growth cone. It is a lamellipodium that protrudes and withdraws numerous filopodia in a rapid pace. The growth cone senses molecular cues from the environment and determines the proper direction of growth for the neurite. The cues can be soluble molecules, components of the extracellular matrix, or cell surface molecules. The growing microtubulin cytoskeleton extends the length of the neurite as it grows, and actin cytoskeleton controls the shape of the growth cone (Purves et al., 2008; Aeschlimann, 2000; Jan & Jan, 2003; Graham & van Ooyen, 2006). Axonal growth cones are bigger than dendrites', and they also grow faster (de Lima et al., 1997).

When the growth cone of an axon encounters a potential target, it expands and extends several filopodia to probe the target area. When suitability of the target is determined, synapse formation can be initiated. The cues sensed by the growth cone can also promote retraction of the neurite, if they indicate an environment

unsuitable for the growing axon. Using these mechanisms, the neurons develop an axonal and dendritic arborization that is typical for their particular neuronal type, and form a highly interconnected cellular network through synapses. Especially the complexity of the dendritic tree determines how many axonal connections from other neurons a neuron can have (Purves et al., 2008).

2.1.2 Development and organization of the neocortex

Development of the cerebral cortex occurs in stages that take place in spatially separated regions of the cortical anlage of the developing animal. In the first stage, a large pool of precursor cells proliferates in the neuroepithelium and subventricular zone. In the second stage, these precursors start to differentiate and migrate into the intermediate zone. In the third stage, the neurons settle in the future cerebral cortex, which is at this point composed of the primordial plexiform layer and the cortical plate. This is the place of final differentiation of the neurons, where they start forming a neuronal network through synapses. These developmental processes have been actively studied along past decades, but many aspects of the development of cortical neurons and the neuronal circuitry are still unknown (de Lima et al., 1997; Rakic, 2002; Mason, 2009; Higginbotham et al., 2010).

The adult cerebral cortex is comprised of tree major parts: neocortex, archicortex and paleocortex. The archicortex and paleocortex are phylogenetically older parts of the cortex, and include regions of the parahippocampal gyrus, hippocampus and olfactory cortex (Purves et al., 2008; Clowry et al., 2010). This thesis focuses solely on the neocortex, leaving the other parts of cerebral cortex out of its scope.

The neocortex is composed of six layers, numbered I to VI, which can be subdivided further (indicated with lower case letters). It is formed in an inside-out manner through cellular migration. Layer VI forms first through asymmetrical divisions of neuronal precursor cells, which are left to reside under the newly formed layer VI. This is followed by generation of layer V neurons from the precursor pool, and the subsequent migration of these cells through layer VI to rest on top of it. Each subsequent layer is formed in a similar manner by division of the precursors in the bottom, followed by their migration through the previously formed layers. Once the six-layered structure is established, growth of neurites begins. In the beginning, an excess of connections is formed, and later the synapses and neurites are pruned to form a network with proper connectivity structure. (Purves et al., 2008; Gilmore & Herrup, 1997; Rash & Grove, 2006; Clowry et al., 2010)

2.1.3 Classification of neocortical cell types

The two major classes of neurons of the neocortex are projection cells, which have very long axons forming connections over long distances, and interneurons, which have shorter axons and are part of the local circuitry. The neurons can be grouped by the appearence of their dendrites to spiny neurons and sparsely spiny or aspiny neurons. In addition to neurons, there are also three different classes of glial cells in the neocortex (and the brain in general): astrocytes, oligodendrocytes and microglia. Astrocytes participate in the maintenance of neuronal circuits by helping to maintain a proper chemical environment and providing assisting metabolism. Oligodendrocytes are responsible for myelination of axons in the CNS, which increases the axons' conducting velocity. Microglia serve the function of macrophages in the CNS. (DeFelipe et al., 2002; Purves et al., 2008).

Over the years, mature neurons of the neocortex have been morphologically classified in several ways, and the division into cell types is still under constant discussion. One way of classifying, based on the appearence of the cells under a microscope, is the division of into subpopulations of pyramidal-like, fusiform and multipolar cells (reviewed by Kriegstein & Dichter, 1983). This classification is based on the shape of the soma, appearence of the dendrites, and density of spines on the dendrites. It can be argued, however, that because the knowledge about neuronal subtypes is still very limited, this morphology-based classification might well prove to be coarse and inadequate. Since this is a commonly used classification in experimental works concerning neuronal single cell development, it will be used in this work. Presently, methods for detailed, molecular level classification of neurons are being developed (Bernard et al., 2009).

Functionally neurons are divided into two classes: excitatory and inhibitory. Excitatory neurons cause an increased probability of action potential firing in their axonal target neurons. Conversely, inhibitory neurons decrease this probability. Excitatory neurons of the neocortex can be roughly considered to have either pyramidal or stellate morphology. These share the characteristics of having spiny dendrites, making asymmetric synaptic contacts on their targets, and using glutamate as their main excitatory neurotransmitter. Inhibitory neurons are varying in shape, but share some morphological characteristics, such as smooth or sparsely spiny dendrites, and formation of symmetric synapses on target cells. Inhibitory neurons mainly use GABA as the neurotransmitter (DeFelipe et al., 2002, and reviewed by de Lima & Voigt, 1997). A feature of special interest in GABAergic transmission is that even though GABA is an inhibitory neurotransmitter in the adult CNS, it acts as a

trophic factor and an excitatory neurotransmitter in the immature nervous system. (Kato-Negishi et al., 2004; Purves et al., 2008). This implies the same circuitry can behave differently in different developmental stages.

2.1.4 Choice of model organism and cell harvesting period

Studying the development of neocortical networks limits the choice of animals suitable as model organisms. Since the neocortex is solely a mammalian speciality, "simpler" animals such as the popular model organism *Drosophila melanogaster* cannot be used for this kind of research. On the other hand, animals very close to human are especially due ethical issues considered very complicated and often undesired for experimental use. The rat *Rattus norvegicus* is, as a mammal, suitable for neocortical research, since all mammals share the essential basic features of neocortical development and neuronal network formation. Because of its small size, easy breeding and less restrictive ethical issues, it has been widely used in research of neocortical function. This has resulted in a wealth of available experimental data about rat neocortical biology.

Very few or no synapses can be observed prenatally in the cortical plate of many mammals (de Lima et al., 1997). This makes the late prenatal period an especially suitable stage for harvesting cells for *in vitro* studies of neuronal network development. Also, both mechanical and biochemical conditions favor the late prenatal (or early postnatal) period for collecting the tissue. In general, the later in development the cells are harvested, the less likely they are to survive (reviewed by Marom & Shahaf, 2002). Higher level of specialization makes it more difficult for the neurons to adapt to their new environment on the culture dish.

2.2 Growth of rat primary neocortical neurons *in vitro*

2.2.1 Preparation of rat neocortical cell cultures

The primary neocortical cultures are typically prepared from E16 or E18 rat pups (see *e.g.* Ichikawa et al., 1993; de Lima et al., 1997). The mother is anesthetized and the pups are collected, and their neocortices extracted. The neocortical tissue is enzymatically digested and then mechanically carefully dissociated to form a cell suspension. Dulbecco's Modified Eagle Medium (DMEM) is typically used, with a

varying composition of additional chemicals. The cells are then plated in a density that depends on the type of experiment to be performed. For morphological studies, lower densities are usually used. It needs to be noted, though, that neuronal growth suffers from low plating densities (*e.g.* van den Pol et al., 1998). Cultures can be expected to show healthier neuronal behavior in cell densities well above the minimum for survival. Plating densities in the studied literature are listed in Table 2.3. Table 2.5 shows how cell density affects growth rates of neurites.

Coating of the plate changes according to preferences in experimental protocols (see *e.g.* Ichikawa et al., 1993; de Lima & Voigt, 1999; Kato-Negishi et al., 2004). Typically used coating agents include collagen, polylysine and polyethyleneimine. Combinations of coating agents used in the referred literature can be found in Table 2.1. Different substrates have differing effects on neuronal growth (Teppola, 2008). It has been shown that laminin-coated plates causes clustering of the neurons. De Lima et al., 1997 concluded that neuronal cultures have more cortical-like features when cultured without laminin.

Because the exctracted neocortical tissue contains all cell types that were present in the brain, also the cell cultures contain glial cells in addition to neurons (Marom & Shahaf, 2002). If no specific action is taken, the glia will proliferate in the culture, and form a layer on top of the neurons. They are beneficial to the well being of neurons, but might obstruct studying the neurons. Therefore, the glia are often eliminated from the culture when formation of neuronal networks is studied. The mitotic inhibitor cytosine arabinoside (Ara-C) is often used to eliminate the proliferating glial cells, but it is also harmful to neurons (de Lima et al., 1997; de Lima & Voigt, 1997, 1999). Additionally, the neurons will suffer from losing the metabolic support provided by the glia, and this problem has to be solved in some way.

If glia are removed from the neuronal culture, a glial coculture can be prepared to aid neuronal health. The coculture's function is to support the metabolism of the neuronal culture and suppress the potential cytotoxicity of the excitatory neurotransmitter glutamate. The astroglial cocultures are prepared in advance to the neuronal cultures.They are usually prepared from newborn to 3 days old rat pups from the cerebral hemispheres of the pups. The glial cells are plated and placed close to the neuronal culture in the same medium, but are kept from direct contact with the neurons (de Lima et al., 1997; de Lima & Voigt, 1999). If a glial coculture is not used, the medium can be supplemented with supportive nutrients. However, this was principally not the case in the literature studied for this work. Table 2.1 shows how the glia have been treated in the studied literature.

2.2.2 Growth of the cultures

With the development of molecular biology techniques, the weight of cellular biology research has moved towards the molecular scale. Therefore the majority of morphological developmental studies date back in time to 1980's and 1990's (Mason, 2009). A good part of the following data is thus from these earlier studies, but has been fortified by more recent findings and reviews also cited below.

Initial growth. Many neurons are probably highly, if not terminally, differentiated at the moment of their plating. They are suspected to have already formed their sub-type idendity *in vivo* before the time of extraction, and to be continuing their growth in this previously established mode after plating (Kriegstein & Dichter, 1983). Neurons have also probably established polarity before they extend their neurites, and this polarity is possibly inherited from the neuroepithelium (Jan & Jan, 2003). The neurons might have small neurites at the time they are extracted, but they lose these when the neocortical tissue is dissociated (Jaap van Pelt, personal communication).

Neurons often present distinct morphological features already after 1 day *in vitro* (DIV), making classification possible. They keep to the morphology they aquired, and these morphological distinctions are probably preserved from the earliest stages of differentiation (Kriegstein & Dichter, 1983). The morphological features of different cell types will be described later in this section.

More than 60 percent of the plated neurons are mitotically active during the first two days (de Lima & Voigt, 1999). Only after the fourth DIV most cells have stopped dividing. This is the point where the glia are usually removed from the culture by treating it with Ara-C. The number of neurons after 7 DIV exceeds the number of plated neurons about tenfold. The majority of the neurons that form a synaptic network are generated within the first 48 hours. During the second week *in vitro* the total cell density starts to decline due to apoptotic cells, even though cell proliferation continues at least until 12 DIV. Glial coculture significantly inhibits proliferation of neuronal precursors in the cell culture.

Axonal growth. The first neurites in the plated neurons are already observed within hours after plating. One of the several primordial neurites of a neuron begins a phase of rapid growth before the others. This neurite will always become the axon. Within the first day after plating, during the initial axon growth phase, the neuron's other neurites do not grow (de Lima et al., 1997; Aeschlimann, 2000). The progression of axonal growth is presented in Table 2.8.

Actin and microtubule dynamics play a role in selecting the neurite that becomes an axon (Jan & Jan, 2003). Changes in the cytoskeleton of the developing neuron are probably induced by the surroundings of the neuron, and thus the axon forms in the appropriate orientation. Mature mammalian CNS neurons lose their ability to regenerate axons. This might be due to an irreversible switching from axonal growth mode to dendritic growth mode by the neuron. Substrate molecules have been shown to influence axon selection, preference being laminin or neuron-glia cell adhesion molecule (NgCAM) over polylysine.

The rate of axonal branching varies between cell types. In large aspinous multipolar cells axons tend to branch extensively. Large aspinous fusiform cells often have several long axon branches and relatively little high order branching. Pyramidal cells, on the other hand, often have axons that give off arcades of collateral branches (Kriegstein & Dichter, 1983; Braitenberg & Schz, 1998).

The decision about which neurite becomes the axon may be influenced by the vicinity of other cells. Axons tend to grow away from the immediately neighboring cell bodies, and out of their cell cluster of origin (de Lima et al., 1997). They often travel in axon bundles between cell clusters. Usually they are not clearly oriented toward a neighboring cluster (Kriegstein & Dichter, 1983; Butz et al., 2009).

Emergence of dendritic trees. Dendrite development is a much less well understood process than axonal development. Both intrinsic and extrinsic processes play a role in shaping the dendritic tree. Some extrinsic factors are common to both axons and dendrites, but affect them differently (Jan & Jan, 2003). Dendritic growth starts around 2-3 DIV. During 4-7 DIV, most of the neurons have a differentiated dendritic tree up to the fourth degree of ramification (de Lima et al., 1997). In isolated cells, dendritic growth is slower than in more densely populated areas. Cells grown in a rich network of fibers develop a more complex dendritic tree (de Lima et al., 1997). Spiny multipolar and pyramidal cells branch more than aspinous multipolar and bipolar cells (Kriegstein & Dichter, 1983). Many dendrites often follow the orientation of axons, or run perpendicular to axonal bundles (de Lima et al., 1997).

When a dendrite bifurcates and branches, only a subset of the new extensions become stable (Jan & Jan, 2003). The building materials for the extensions are manufactured both in soma and the dendrites. There are several recognized extrinsic guidance cues for dendritic growth and branching. Presumably, different neurons can respond differently to the same extracellular cues due to their intrinsic differences. Transcriptional regulators could be the mediators of type-specific dendritic

morphology. The transcriptional programs could affect the wiring of neuronal networks through dendritic (and possibly also axonal) targeting. Neurons with distinct dendritic morphology typically perform different signal processing and computations for their particular physiological functions.

Some subtypes of neurons show the tiling phenomenon, which means a complete but nonredundant coverage of a receptive area by the dendrites of the same functional group of neurons. This is likely to be a fairly general organizing principle in the nervous system. The cellular basis of tiling seems to be a like-repels-like type of interaction, both hetero- and isoneural. The molecular mechanisms of tiling should have a bidirectional quality. They could be based on contact-mediated interaction between neurites, or on a short-range diffusible cue (Jan & Jan, 2003; Mason, 2009).

Features of neuronal development in the culture. The sequence of differentiation of neuronal features is always as described previously, but the timing and long-term differentiation depends on growth conditions. Local cell density affects the pace of development. Higher cell densities have been shown to speed up development. The pace of development is also affected by substrate quality, higher quality substrate speeding up the pace. During the first week *in vitro*, the substrate quality affects growth and survival of the neurons. Most effects of initial cell density might be transitory, because the cell density is dynamically regulated during long-term cultivation (de Lima et al., 1997; Wagenaar et al., 2006).

Cells in denser areas have longer and faster-growing neurites than cells in sparser areas. Neurite growth is three times faster in the dense areas (cell-to-cell distance about 5 μm) than in the sparse ones (cell-to-cell distance about 25 μm). Also, cells growing on heat-killed neurons demonstrate faster growth and longer neurite length. The effect cannot be explained by changes in growth factor concentrations, although they might play a role. This suggests that contact between cells might play a significant part in determining the rate of neurite growth, possibly through molecular interactions between cell surfaces, since no live and trophic factor secreting cells are required for this effect (van den Pol et al., 1998).

In the final stages of the culture, axons and dendrites can extend over 1 mm. This kind of a culture typically contains a network of about 150 000 neurons in an approximately 300mm^2 area. (Marom & Shahaf, 2002)

Formation of synapses. In the culture synapses are morphologically recognized from presence of pre- and postsynaptic membranous densities, the synaptic cleft, and synaptic vesicles. An immature synapse can also be recognized in the culture from less clear pre- and postsynaptic membrane densities, shorter synaptic contact zone

and a smaller number of synaptic vesicles. Also, a postsynaptic density without a presynaptic counterpart or neurites without a presynaptic structure can be observed (Ichikawa et al., 1993; Harris, 1999; Hering & Sheng, 2001).

Between 5-25 DIV, there is a rapid increase in the number of synaptic structures with a mature morphology (Marom & Shahaf, 2002). Many neurons are synaptically coupled already at 3 DIV, and most neurons are coupled at 4 DIV (van den Pol et al., 1998). However, Ichikawa et al., 1993 did not observe any synapses at 3 DIV, and those that were observed at 7 DIV had an immature morphology. This is probably due to differences in preparation and culturing protocols. Progression of synapse formation is presented in Tables 2.6, 2.7 and 2.9.

During the initial days of growth in the cultures, there is a delay in synapse formation between axons and dendrites that have grown physically close to each other. This seems to be due to the inability of the immature dendrites to form postsynaptic specializations. The axons probably have the ability to form the necessary presynaptic area and seem to be able to form synapses from a very early stage, but the young dendrites seem to take a bit longer time to mature and be able to form the postsynaptic site (de Lima & Voigt, 1997; van den Pol et al., 1998).

Cell density is a critical factor for synaptogenesis, and also for survival of neurons (van den Pol et al., 1998; Marom & Shahaf, 2002). It determines the distance to the axons' targets, which in turn determines the time it takes for the axons to find appropriate postsynaptic targets (van den Pol et al., 1998). Cells grown in plating densities of less than 100 cells/mm^2 tend to stay isolated, but with densities higher than that, contacts with neighbors are made quickly and synapses are formed. The beginning of synaptogenesis coincides with the beginning of dendritic growth. The density of putative synaptic boutons increases significantly at least until the end of third week *in vitro*, despite the concominant decrease in cell density (de Lima et al., 1997). High cell density may facilitate synapse formation and development of action potential firing and related molecular functions. Synapses are three times more frequent in the dense areas (cell-to-cell distance about 5 μm) than in the sparse ones (cell-to-cell distance about 25 μm) (van den Pol et al., 1998).

Developing neurons often show spontaneous synaptic activity. However, some developing neurons seem to have silent synapses. In high density cultures, but not in low-density ones, electrical stimulation of the presynaptic neurons often activates and thus reveals the synapses that do not present spontaneous activity (van den Pol et al., 1998).

As the cortical culture matures, overall synaptic number declines during weeks 4-10

in vitro. In the networks at their mature phase, each neuron is connected monosynaptically to 10-30% of all other neurons (*e.g.* Jimbo et al., 1999, reviewed by Marom & Shahaf, 2002). The synaptic transmission delay between a neuron and its randomly chosen "partner" in the culture corresponds to 1-10 "jumps" through a synapse between the two cells, and the delay has no obvious correlation to the distance between the pair (van den Pol et al., 1998).

2.2.3 Cell types and their morphology *in vitro*

Distribution of cell types *in vitro* resembles that *in vivo*. Most of the neurons are excitatory glutamatergic cells, 10-25% are inhibitory GABAergic, and 2-3% are acetylcholinergic (de Lima & Voigt, 1997; Marom & Shahaf, 2002; Kato-Negishi et al., 2004). Table 2.4 shows experimentally determined percentages of different neuronal cell types in the culture. Morphology of neocortical cells in the culture largely resembles their counterparts in the brain. Even confined in the limited dimensions of the culture, the neurons have distinguishable features (Kriegstein & Dichter, 1983).

In a cell culture, pyramidal cells have a triangular cell body, one prominent apical dendrite and several shorter basal denrdites. The dendrites bear many spines. Cultured fusiform cells have a soma that is often spherical, and either spiny or aspinous dendrites that emerge from opposite sides of the soma. By the number of the emerging dendrites, fusiform cells are further divided into bipolar cells, which have single dendrites emerging from opposite sides of the soma, and bitufted cells, which have several dendrites on the opposite sides. Finally, cultured multipolar cells have multiple dendrites of approximately equal length appearing from various sites on the soma (Kriegstein & Dichter, 1983).

Axons in the cortical cells often originate near the origin point of a dendrite on the cell body, or as a branch off the proximal segment of a dendrite. Multiple axons are typically not present in one cell (Kriegstein & Dichter, 1983). This is also a feature of *in vivo* neocortical cells.

2.3 Modeling the growth of neocortical neuronal cultures *in silico*

2.3.1 What is a model?

When biologists talk about models, they often mean model organisms. The model organism is used as a system that can be characterized and altered to study a certain phenomenon. The organism is then called a model of this phenomenon. However, when computational scientists talk about models of biology, they mean mathematical descriptions of biological phenomena (van Pelt & Uylings, 2005). In these models, biological knowledge is expressed through mathematical formulation. The models are simulated in a computer to obtain data about their dynamics (time-series behavior). Models are a theoretical and computational tool for implementing the current knowledge and hypotheses about the system quantitatively. This is the goal of computational neuroscience (Sejnowski et al., 1988). The simulation results are compared against experimental results, and the model is tuned to produce as biologically realistic results as possible. A good computational model could be thought of as a biological laboratory *in silico*. Modeling enables the study of the system, and a succesful model also allows new testable predictions about the system to be made. Sometimes models are needed to study a system from a point of view which is not easily accessible by experimental means (van Pelt & Uylings, 2005).

Computational modeling can be done on many levels. One could for example model the chemical reactions of a molecular reaction pathway, interactions between cells, or the functioning of a whole organ. These are examples of models of different scales. If a model spans two or more scales, it is called a multiscale model (Sporns et al., 2005). In the case of cell biology, this could be a model that not only models in detail some chemical reaction pathways inside cells, but also the behavior of a whole population of cells when they signal to each other using these pathways. In this work, single scale models on the level of a network of cells are utilized.

2.3.2 Modeling biological systems

The question of how neurons acquire their morphological characteristics during development is a complicated one. Not only are the possible outcomes of neuritic shapes extremely diverse, but the process is also very dynamical and depends on many extrinsic and intrinsic factors. To understand such a complex system and its dynamics, theoretical and computational modeling approaches are necessary (van

Pelt & Uylings, 2007). Biological systems show organization on all levels of temporal and spatial scales. Because of their complexity, biological systems represent systems of very high dimensionality, that is, a high number of affecting components. That is why building a model of a biological system requires a carefully planned approach to reduce the dimensionality to a level that is still treatable computationally, but produces meaningful information which can be interpreted in a biological way. This calls for making well thought out approximations (see *e.g.* van Pelt & Uylings, 2007).

The way and extent to which approximation is done depends strongly on the particular research question being studied (Sejnowski et al., 1988; van Pelt & Uylings, 2007). One typical method of approximation is to combine many degrees of freedom into one probability function and regard the system as stochastic, i.e. such that the possible outcomes of the development of the system are not deterministic, but behave in a probabilistic way (White et al., 2000; Saarinen et al., 2008). If one wants to approximate as little as possible, the approach is to integrate all available knowledge of the system to study its fine details. In this case, there is a danger that the model itself is too complex to be understandable.

In the case of the human nervous system, the whole system comprises all the phenomena from the molecular level up to cognitive skills and behavior. Even though our knowledge of this system is still very limited, at our current level of understanding of biological systems and modeling techniques, integrating all available information in detail might not be the most feasible way to study neuronal systems. A model with a very high number of components would be difficult to control as the number of variables is too great, and so the biological meaning of obtained results would be difficult, if not impossible, to interpret. Therefore, it should be determined what kind of information is wanted out of the model, and what can be approximated. Based on this, it should be decided how the processes affecting the phenomenon of interest are added to the model in a level of detail that is sufficient. This way the problem can be approached in a piecewise manner (van Pelt & Uylings, 2005, 2007).

2.3.3 Approaches to modeling the structural growth of neuronal networks

The model for producing neuronal network morphologies can be either a reconstruction model or a growth model. The reconstruction model approach uses experimentally obtained distribution functions to describe neuritic shape parameters, and dendritic structures are generated by random sampling of these distributions. This

approach generates "ready made" networks in their final stage, with no regard for the developmental stages through which the end result was obtained. As such it is suitable if representative networks are to be generated *in silico*, but information about the stages of growth is not required. The growth model approach, on the other hand, aims at modeling the growth of neurites from the principles of neuritic development. This approach models the processes behind neuritic elongation and branching, and through several intermediate immature developmental stages produces a mature network. Thus, growth model is the approach suitable for studying the principles behind the development (Ascoli et al., 2001; van Pelt & Uylings, 2005; Bekkers & Häusser, 2007; Cuntz et al., 2010).

The final shape of neurites is determined by the rate of neurite elongation, retraction and branching, growth direction, path finding and competition for resources(van Pelt & Uylings, 2005; Kiddie et al., 2005). Therefore, these are the key features to be modeled. Elongation requires the polymerization of tubulins to add to the microtubule cytoskeleton at the tip of the growing neurite, and depolymerization of tubulins leads to retraction of neurites. A neurite bifurcates by splitting of a the growth cone, including its microtubule cytoskeleton, into two separate branches growing on their own. The growth cones might also change the orientation of their growth. A variety of mechanisms regulates the behaviour of the growth cones, such as local extracellular cues, receptor-mediated transmembrane signaling, intracellular factors, and bioelectrical activity. Production and transportation times (mainly of tubulin) along the neurite also affect the growth process. Limited resources might result in a competition between growth cones or axons. Because of this large number of factors affecting the growth process, the complete picture of neurite growth is quite complex to model (van Pelt & Uylings, 2005; Kiddie et al., 2005).

Growth can be modeled biophysically or phenomenologically (Butz et al., 2009). Biophysical models aim at understanding systems from the point of view of how their physical and chemical properties define their functioning, and thus can include a variety of molecular level details. A biophysical model of neurite growth aims to include some or all of the details described in the previous paragraph in the form of chemical reaction pathways. Phenomenological models, on the other hand, model the growth from the point of the end result, without describing the mechanisms that control the phenomenon. In the case of growth of neuronal networks in the context of this work, the end result is the change in neuronal morphology and distributions of synapses in the network. When modeling neuronal growth, this approach aims at finding the proper algorithms to describe the behavior of growth cones directly in terms of elongation and branching rates. Because there is such a large number

of (often poorly known) processes involved in the behavior of growth cones, one reasonable approach is to model the behavior of growth cones as a stochastic process. In this way, the probability function is considered to include all the fine details of regulation that cannot be modeled as such, but will exert their influence through shaping the probability function (White et al., 2000; van Pelt & Uylings, 2005; Saarinen et al., 2008).

Topology of a dendritic tree or axonal arbor. The shapes of dendrites and axons have to be parametrized in order to model the growth, *i.e.* the complex shapes have to be reduced to a set of well-defined parameters. These parameters include the number of branch points in the dendritic tree or axon, number of segments, length of the segments, connectivity pattern of the segments which will give out the topology of the tree, diameter of the segments, curvature of the segments and their embedding in space. The numerical values for these parameters have to be determined experimentally for the type of neuron and conditions to be simulated (van Pelt & Uylings, 2005, 2007).

2.3.4 Obtaining parameter values for the models

Parameters for the models are obtained by observing living neurons. The essential features of the growth of neurites, such as speed of elongation of axons and dendrites, bifurcation of growth cones, and growth directions, have to be quantified. There is a lot of data available about neuronal growth and morphology *in vivo* (*e.g.*, at www.neuromorpho.org), and the existing simulators largely use this data to generate neurons and networks whith realistic morphologies.

However, because growth conditions are very dissimilar in the living brain and in a dissociated cell culture on a dish, the parameters obtained from *in vivo* experiments are not guaranteed to be directly applicable for simulating growth on a culture dish. To model growth in a cell culture, many of the parameters should be obtained from cell culture experiments. To find values for parameters to simulate models of *in vitro* growth, numerical data about neuronal growth *in vitro* was extracted from a multitude of sources in the literature. The following set of tables presents the found data, on which to base the parameters in simulations.

Author	**Day**	***In vitro***	**Glia**	**Substrate**	**Content**
Kriegstein & Dichter, 1983	E15	x	?	collagen + PL	Morphological classification of neurons.
Ichikawa et al., 1993	E18	x	(+)	PLL	Formation and maturation of synapses.
de Lima et al., 1997	E16	x	+(+)	PDL, PDL + laminin	Development of neurites and synapses; morphology; glial contribution.
de Lima & Voigt, 1997	E16	x	(+) –	PDL	Identification of two GABA populations.
van den Pol et al., 1998	E18	x	–	PL	(hippocampus & hypothalamus) Role of axon target distance.
de Lima & Voigt, 1999	E16	x	+ –	PDL, PDL + glia, PDL + glia (dead)	Astroglia inhibit the small GABAergic population.
Potter & DeMarse, 2001	E18	x	(+)	PEI + laminin	Methods for long term culturing.
Lesuisse & Martin, 2002	E16	x	(+)	PDL	Signs of health and aging in mouse long term cultures.
Marom & Shahaf, 2002 (review)	E, P	x			Development, learning and memory in large networks.
Jan & Jan, 2003 (review)	-				Molecular control of dendritc development.
Kato-Negishi et al., 2004	E18	x	(+)	PEI	Developmental changes of GABAergic synapses.
Wagenaar et al., 2006	E18	x	(+)	laminin	Development of bursting patterns.
Bernard et al., 2009 (review)					New approaches for classifying neurons.

Table 2.1: The most important studied experimantal publications and their culturing protocols. The columns are as follows. Day: the embryonic day when the brain tissue was harvested. E refers to embryonic, and the following number to days after conception. P refers to postnatal. *In vitro*: cross if the study concerns *in vitro* data. Glia: treatment of glial cells in the experiments. + denotes a feeder coculture; (+) denotes that glia were not eliminated; – denotes that glia were completely eliminated. More than one markings indicate that several types of experiments were performed. Subsrate: the type of substrates used. See Abbreviations (page vi) for explanation of abbreviations of substrate names. Content: experimental content of the publication.

Cell size and density

DIV	Type	Diameter (μm)	Density (cells/mm^2)	Reference
0	all	-	∼70	de Lima & Voigt, 1997
	neuron	-	0	de Lima & Voigt, 1997
	GABA	∼7.14-11.28	1	de Lima & Voigt, 1997
	all	-	∼80±60	de Lima et al., 1997
1	all	-	∼210±30	de Lima & Voigt, 1997
	neuron	-	5	de Lima & Voigt, 1997
	GABA	∼7.14-12.26 OR ∼12.87-14.27	∼2±0.5	de Lima & Voigt, 1997
	all	-	∼430±240	de Lima et al., 1997
3	all	-	∼190±110	de Lima et al., 1997
4	all	-	∼290±60	de Lima et al., 1997
	all	-	∼560±410	de Lima & Voigt, 1997
	neuron	-	∼120±30	de Lima & Voigt, 1997
	GABA	∼7.14-10.70 OR ∼9.77-16.35	∼11.5±6.5	de Lima & Voigt, 1997
	all	-	∼1650±230	de Lima et al., 1997
5	all	-	∼330±100	de Lima et al., 1997
6	all	-	∼440±150	de Lima et al., 1997
3-6	GABA	9.4-23.4	-	Kato-Negishi et al., 2004
7	all	9.1 ± 2.0	2440 ± 400	Ichikawa et al., 1993
	all	-	∼425±95	de Lima & Voigt, 1997
	neuron	-	∼385±105	de Lima & Voigt, 1997
	GABA	∼7.14-10.70 OR ∼10.70-15.96	∼1.8±1	de Lima & Voigt, 1997
	all	-	∼1100±280	de Lima et al., 1997
8	all	-	∼350±120	de Lima et al., 1997
11	all	-	∼305±45	de Lima & Voigt, 1997
	neuron	-	∼300±50	de Lima & Voigt, 1997
	GABA	∼7.14-10.09 OR ∼10.70-17.84	∼4	de Lima & Voigt, 1997
	all	-	∼720±300	de Lima et al., 1997
14	all	10.8 ± 2.4	1380 ± 180	Ichikawa et al., 1993
	all	-	∼295±85	de Lima & Voigt, 1997
	neuron	-	∼295±80	de Lima & Voigt, 1997
	GABA	∼7.14-11.28 OR ∼12.62-19.54	∼2.5±1	de Lima & Voigt, 1997
	all	-	∼550±250	de Lima et al., 1997
21	all	11.1 ± 3.8	910 ± 330	Ichikawa et al., 1993
	all	-	∼155±40	de Lima & Voigt, 1997
	neuron	-	∼150±40	de Lima & Voigt, 1997
	GABA	∼7.14-11.28 OR ∼20.81	∼3±0.5	de Lima & Voigt, 1997
	all	-	∼410±10	de Lima et al., 1997
28	all	13.2 ± 2.7	360 ± 80	Ichikawa et al., 1993
35	all	12.1 ± 3.0	410 ± 90	Ichikawa et al., 1993

Table 2.2: Reported cell diameters and densities. In the column "Type"; All: all cells on the plate. Neuron: neuronal cells. GABA: gabaergic cells. In the column "Diameter"; Two different diameter ranges separated by 'OR' represent two populations of cells of different sizes in the cultures. About the data from de Lima & Voigt, 1997: The data is from one example set of cultures, where Ara-C was added at 4 DIV.

Plating densities

cells/mm^2	Purpose of the study	Reference
∼330	Study of morphology	Kriegstein & Dichter, 1983
unknown	Study of synaptogenesis	Ichikawa et al., 1993
20-100 100-300, 300-1500	Events associated with neuronal development Analysis of axonal network formation and synaptogenesis	de Lima et al., 1997
50-1500	Study of development of GABAergic cells	de Lima & Voigt, 1997

Table 2.3: Reported plating densities and the intended purpose of those cultures.

Presence of cell types

Neurotransmitter		Morphology				Reference
GABA	**AChol**	**Pyram.**	**Fusif.**	**Multip.**	**Unk.**	
		26 %	30 %	39 %	6 %	Kriegstein & Dichter, 1983
	2.64±1.73 %					de Lima & Voigt, 1997
10-25 %	2-3 %					Marom & Shahaf, 2002
10.2 % (6DIV) - 15.8% (10DIV)						Kato-Negishi et al., 2004

Table 2.4: Presence of different cell types in neuronal cultures as reported by different authors. Division by neurotransmitter type: GABA: GABAergic neurons; AChol: acetylcholinergic neurons. The rest can be assumed to be mainly glutamatergic neurons. Division by morphology: Pyram.: pyramidal neurons; Fusif.: fusiform neurons; Multip.: multipolar neurons; Unk.: neurons of unknown morphology.

Neurite growth rates (van den Pol et al., 1998)

Culture type	Distance between cells	Growth rate of neurites
sparse	20 μm	3.6 μm/h
dense	5 μm	5.8 μm/h

Table 2.5: Growth rates of all neurites neurites reported in sparse and dense culture experiments. Here, axons and dendrites were not distinguished from each other.

Density of GABAergic synapses (Kato-Negishi et al., 2004)

DIV	Number of synapses per 10 μm of dendrite
10	1.13 ± 0.13
15	3.03 ± 0.21
20	3.77 ± 0.33

Table 2.6: Density of GABAergic synapses per 10 μm of dendrite length at different time points of culturing the cells.

Number and density of synapses (from Ichikawa et al., 1993)

DIV	Experiment	Synapses / neuron	Synapses / 10^4 μm^2	Synapses / 10^6 μm^3
3	M86			∼0
	M95			∼0
7	M86			∼1800
	M87			∼1600
	M92			∼1900
	M93			∼1800
	M95			-
	mean	64.1±9.8	54±3.2	1780±86
14	M86			∼3800
	M87			∼2600
	M92			∼6000
	M93			∼5000
	M95			∼3600
	mean	319.5±65.7	128±13.9	4244±595
21	M86			∼1500
	M87			∼4300
	M92			∼1800
	M93			∼4300
	M95			∼1700
	mean	354.7±179.9	85±25.1	2285±647
28	M86			∼3000
	M87			∼2900
	M92			-
	M93			∼3600
	M95			∼700
	mean	1130.1±254.3	89±21.9	2252±646
35	M86			∼1200
	M87			-
	M92			∼2300
	M93			∼3500
	M95			∼1300
	mean	606.9±125.9	86±22.0	2080±532

Table 2.7: Number and density of synapses on different culturing days. The table contains results from different individual experiments and the mean values over all the presented experiments.

Axonal density (from de Lima et al., 1997)

DIV	Axonal density (coverage percentage of plate area)
3	∼3 ±1 %
4	∼8 ± 3 %
5	∼11 ± 3 %
6	∼31 ± 4 %
7	∼38 ± 2 %
8	∼51 ± 7 %

Table 2.8: Axonal density at different time points measured by the area of the plate covered by axons.

Progression of synapse formation

DIV	Day	Synapses /$10^4 \mu m^2$	Synapses /$10^6 \mu m^3$	State of synapses	Author
3	E18	0	0	No synapses	Ichikawa et al., 1993
4	E16			Synaptic terminals first observed.	de Lima et al., 1997
7	E18	54 ± 3.2	1780 ± 386	Many synapses with immature morphology. Pre- and postsynaptic densities not very clear. Synaptic contact zone shorter. Smaller number of synaptic vesicles. Vacant postsynaptic densities and neurites without postsynaptic structure present.	Ichikawa et al., 1993
14	E18	128 ± 13.9	4244 ± 595	Synaptic density and nubmer of synapses per neuron significantly increased. Number of synaptic vesicles increased. Synaptic contact zone fairly short.	Ichikawa et al., 1993
21	E18	85 ± 25.1	2285 ± 674	Synaptic density begins to vary between cultures. Synaptic contact zone size, number of synapses per neuron and number of synaptic vesicles increased. Synaptic morphology resembles that in adult rat brain.	Ichikawa et al., 1993
28	E18	89 ± 21.9	2552 ± 646	Synaptic contact zone size increased. Number of synapses per neuron at peak. Synapses observed frequently on spines.	Ichikawa et al., 1993
35	E18	86 ± 22.0	2080 ± 532	Number of synapses per neuron cut to almost half of 28 DIV, synaptic density lower than on 14 DIV. Synaptic contact zone and vesicle number increased. Synapses observed frequently on spines.	Ichikawa et al., 1993

Table 2.9: Progression of synapse formation in the neuronal culture. Two different density measures are presented (synapses per ten thousand square micrometers and synapses per one hundred thousand cubic micrometers). A description of synaptic morphology is also included. In the column "Day": The time of tissue harvesting. E refers to embryonic, and the following number to days after conception.

3 Aims of the research

The aim of this M.Sc. thesis is to test and evaluate two recently published simulation tools, CX3D (Zubler & Douglas, 2009) and NETMORPH (Koene et al., 2009b). To this end, a morphological model of neuronal growth *in vitro* including synapse formation will be constructed. The parameter value ranges for this model will be chosen based on the studied literature. This model will be simulated, and the produced networks will be quantified based on Sholl analysis and graph theoretical measures. The results on network growth will be compared to existing data in the literature. Based on the results and comparison to experimental data, the two simulation tools' capabilities will be assessed. The aims are presented schematically in Figure 3.1

To accomplish the task, this work combines knowledge from the fields of computational and experimental neuroscience, and applies methods from the fields of mathematics, computer science, graph theory, and scientific computing.

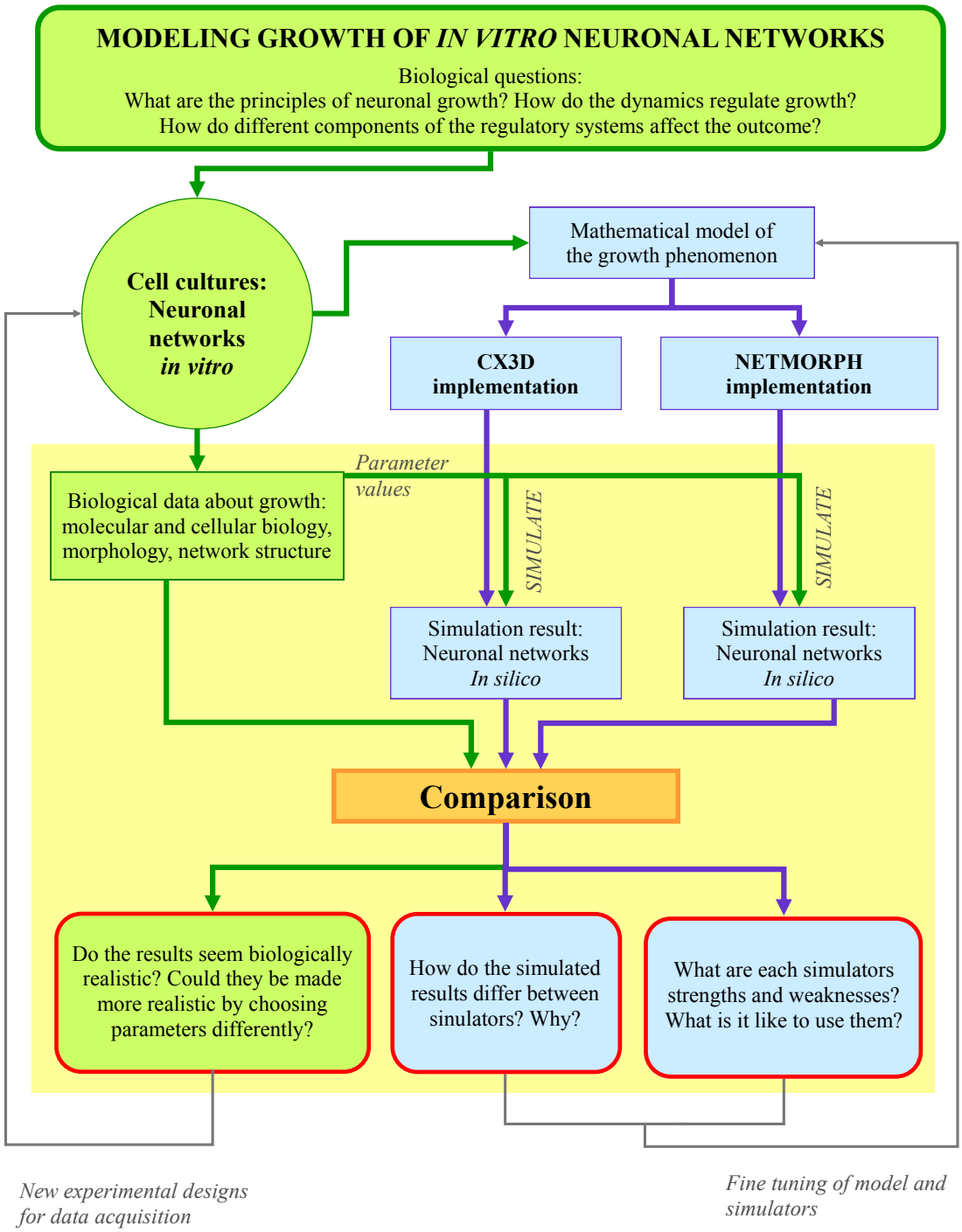

Figure 3.1: An overall representation of the aims of the thesis, and its background and intended usability. Yellow background color defines the area of the thesis. Boxes with red outlines represent questions for which answers are sought. Green boxes and arrows represent biological experiments and data. Blue boxes and arrows represent computational experiments and data. Grey arrows represent possible future usage of the thesis' results.

4 Methods

4.1 The underlying network growth model

4.1.1 About the choice of a model

The model chosen to be implemented and simulated in the two simulation tools represents *in vitro* growth of neurons. Because of the flexibility and simplicity of the *in vitro* system, it is a desirable way to study development of neuronal morphology and neuronal networks. On the other hand, computational modeling of cell cultures might help to uncover the factors affecting the growth of the studied neuronal cultures.

The chosen model was originally constructed with *in vivo* data, and was shown to reproduce the observed neuronal morphologies well (van Pelt et al., 2001; van Pelt & Uylings, 2002, 2005, 2007). Because the most important features of neurons have been shown to be present also in cell culture (Kriegstein & Dichter, 1983; Marom & Shahaf, 2002), and because the same intrinsic principles guide the formation of morphological features *in vitro* as well as *in vivo*, with some modifications this model can be expected to represent also growth in clutures.

The model has been selected so that all main aspects of the model can be implemented in both tested simulation tools. Parameters of the model have been selected so that the simulations should not get too heavy with either of the tools. This facilitates comparison of the two tools.

4.1.2 Model components

The model used to describe morphological development of neuronal cultures has been formulated by van Pelt and co-workers. The development of the model of morphological growth of neuronal networks has been described in *e.g.* van Pelt et al., 2001 and van Pelt & Uylings, 2002, 2005, 2007. The basis of this model are three-dimensional reconstructions of single neuron morphologies. To obtain data for this purpose, the dendritic morphologies of different types of neurons in the brain were quantisized. Van Pelt & Uylings, 2005 summarizes a variety of experimental

work on this topic, listing numerical values of the relevant morphological aspects for several different types of neurons. The model used in this thesis is the one implemented in NETMORPH simulation tool, formulated by van Pelt et al. (Koene et al., 2009b). This model has been validated for many neuronal cell types, and has been shown to accurately describe dendritic metrical and topological variety (van Pelt et al., 2001; Koene et al., 2009b).

Although this model is based on *in vivo* data and thus the neuronal morphologies differ from the *in vitro* situation, it is nevertheless a realistic representation of formation neuronal morphology and neuronal networks in a healthy tissue. Because it is presumable that even in the lack of normal cues of living tissue the neurons on the plate develop according to the same intrinsic set of rules that guide them *in vivo*, adapting this model to the *in vitro* situation is reasonable. In this work, the model is adapted to conform to two-dimensionality.

Van Pelt's growth model considers neuronal growth as a stochastic process in time in which neurites can elongate and bifurcate. The probabilities of these events are defined as functions of time. The basic assumptions of the models are that all neurite tips, which are in essence the growth cones, are assumed to participate in both branching and elongation, and that branching and elongation are independent processes (Koene et al., 2009b). The model components are defined as follows.

Branching probability is the probability, per unit of time, for a branching event to occur at a terminal segment. The probability of a terminal segment j branching at time step $(t_i, t_i + \Delta t)$ into two new terminal segments is

$$p_{i,j} = n_i^{-E} B_{inf} e^{-t_i/\tau} (e^{\Delta t/\tau} - 1) 2^{-S\gamma_j} / C_{n_i},$$

where, n_i is the number of terminal segments in the whole cell at time t_i, E is a constant determining the magnitude of competition, and B_{inf} and τ are constant parameters governing the intensity and slowness of the branching (Koene et al., 2009b; van Pelt & Uylings, 2005). The variable γ_j is the centrifugal order of the terminal segment j, i.e. the number of segments between the soma and the terminal segment, S is a constant that determines the effect of the centrifugal order on the branching rate, and $C_{n_i} = \frac{1}{n_i} \sum_{k=1}^{n_i} 2^{-S\gamma_k}$ is a normalization constant.

Elongation of terminal segments of neurites is described as

$$\nu(t) = \nu_0 n(t)^{-F},$$

where $\nu(t)$ represents the average elongation rate of a terminal segment at time t,

ν_0 is a constant, $n(t)$ is the number of terminal segments in the neuron, and F is a constant parameter determining the level of competition for resources between terminal segments (van Pelt & Uylings, 2005; Koene et al., 2009b).

An **initial length** for daughter segments is set for each new branch after a branching event has occurred. This is done to take into account the observation that although the branching event occurs as a point process in the model, the branching of a real growth cone is a process occurring over a period of time. The addition of initial segments for daughter branches results in accurate reproduction of experimentally observed morphologies after branching events (Koene et al., 2009b). In NETMORPH, the initial length is selected randomly by dividing the last elongated part of the terminal segment. In CX3D, it is set to default 10 μm.

Direction of outgrowth is determined at each time step. The probability of changing growth direction at time $t + \Delta t$ depends on the increase in length of the terminal segment during the time interval $(t, t + \Delta t)$. The new direction depends on the previous growth directions of the considered neurite segment (Koene et al., 2009b).

In NETMORPH, the original method of assigning **branching angles** is implemented so that forces proportional to their initial length are assigned to both daughter branches, and the angle between them is randomly drawn from a given propability distribution function. The new initial segments are drawn in a parallelogram, and the sum vector of this parallelogram is aligned with the parent segment. The plane of branching is then rotated around the axis of the parent segment by an angle randomly selected from a uniform distribution [0, 2π] to produce the final orientation of the two daughter branches (Koene et al., 2009b). However, because in CX3D the branching angles are fixed to 60 degrees, this fixed angle is used in both simulators for our model.

Segment diameters in NETMORPH are assigned to all neurites after the simulation of growth is finished. Assigning diameters is based on empirically obtained values and the observation that segments become thicker as the subtree they support increases its number of terminal segments. The terminal segment diameters in the model are estimated by randomly sampling the experimentally observed terminal segment diameter distribution (van Pelt & Uylings, 2005; Koene et al., 2009b). The diameters of other segments are computed using the power law rule.

In the CX3D implementation the segment diameters are fixed. With each branching event, the diameters of daughter branches are computed using the power law rule. The initial segment length is set so that the outcome of segment diameter widths is

estimated to be similar to that in the NETMORPH implementation.

4.2 The simulation tools

4.2.1 NETMORPH

NETMORPH, by Koene et al., 2009b, is one of the two simulation tools evaluated in this work. The model described in section 4.1 is originally implemented in this tool. NETMORPH is a simulator for modeling the development of large scale neuronal networks with realistic morphologies. The working principle of NETMORPH is to solve equations describing the growth of neurites for chosen parameter values over time. NETMORPH simulates the growth of axons and dendrites, but does not allow mimicking cell division or death, or movement of neurons. The perspective is that of an individual growth cone. Elongation, branching and turning of neurites, mediated by the growth cones, are described in a stochastic, phenomenological manner. The description of growth includes influence of a growth cone's positions in its dendritic tree and how the position affects its growth, and the influence of competition for resources between different growth cones of a neurite. Synapses can be formed between an axon and a dendrite, if they come close enough to each other. NETMORPH is open source software written in C++.

4.2.2 CX3D

The second evaluated simulation tool is CX3D, by Zubler & Douglas, 2009. The authors emphasize the importance of mechanical forces and diffusible factors in modeling the development of tissues, and thus CX3D simulates the biophysical interactions of objects in a three-dimensional physical space, while increasing the length of neurites according to specified rules. CX3D is open source software, written in Java, and intended for modeling all stages of corticogenesis. It enables, for example, modeling cell division and migration, extension of axons and dendrites, and establishment of synaptic connections. The user can specify which processes are included, and at what level of complexity.

The architecture in CX3D is organized in four layers of abstraction. They have been designed so that the user does not have to manipulate all of them to implement a model. The model is coded in the two uppermost and most "biological" layers. The layers are from top down as follows. The cell layer (figure 4.1, ovals) contains a

unique instance for each neuron present in the simulation. It lists a unique label for each neuron (figure 4.1, 'Cell'), and the biological properties of that neuron (figure 4.1, 'CellModule'). These biological properties can include for example the cell cycle, or a gene network expressed in the cell (not implemented in the current version). The local biology layer (figure 4.1, light grey stripe lined boxes) has all the elements that make up the cells: a soma element for each soma (figure 4.1, 'SomaElement'), and a collection of neurite elements for each neurite (figure 4.1, 'NeuriteElement'). Local biological behavior, such as movement, branching, or production or detection of molecular guidance cues are coded in this level. The physics layer (figure 4.1, grey lined boxes with black edges) contains the physical properties of the cells. These include for example volume, friction and elasticity of the cell parts. The physical layer also performs the diffusion processes. Each soma element is associated with an instance of physical sphere (figure 4.1, 'PhysicalSphere'), and each neurite element with an instance of physical cylinder (figure 4.1, 'PhysicalCylinder'). Physical spheres and physical cylinders derive from physical objects, which in turn derive from the abstract physical node (figure 4.1, 'PhysicalObject' and 'PhysicalNode'). A physical node represents a volume of space, and the extracellular substances it holds. When a physical node is a physical sphere or a physical cylinder, the elements within the space are intracellular elements. Finally, the spatial organization layer (figure 4.1, black lined boxes) defines the boundaries between physical nodes, and defines the neighboring relations between physical objects. See figure 4.1 for an illustration of the layer hierarchy, and figure 4.2 for an illustration of how the different layers work in representing cells and the environment.

4.3 The tested models

4.3.1 Model 1: Comparing the simulation tools

The model simulated in both simulation tools is essentially the model in NETMORPH (van Pelt et al., 2001; van Pelt & Uylings, 2002, 2005, 2007; Koene et al., 2009b). Model parameters and features were chosen to accommodate the limitations of both tools.

The number of cells in the simulated network was set to 100, since a larger number of neurons tended to make the simulations too heavy with CX3D. The different cell types included in the simulation were pyramidal cells (80% of cells) and multipolar cells (20%). The simulation space size was scaled so that the average density of cells was 100 cells/mm^2. In pyramidal cells, 2-5 basal dendrites were initiated on

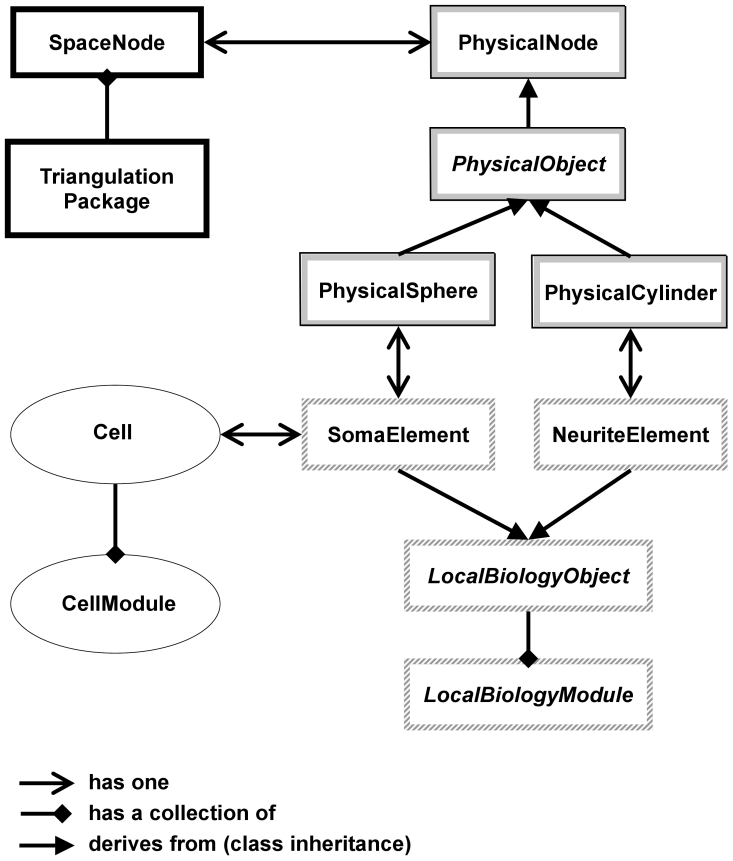

Figure 4.1: The architecture of the layers in CX3D. The spatial organization layer is in black lined boxes, the physical layer is in grey lined boxes with black edges, the local biology layer is in light grey stripe lined boxes, and the cell layer is in ovals. Figure modified from the CX3D tutorial (Zubler, 2009).

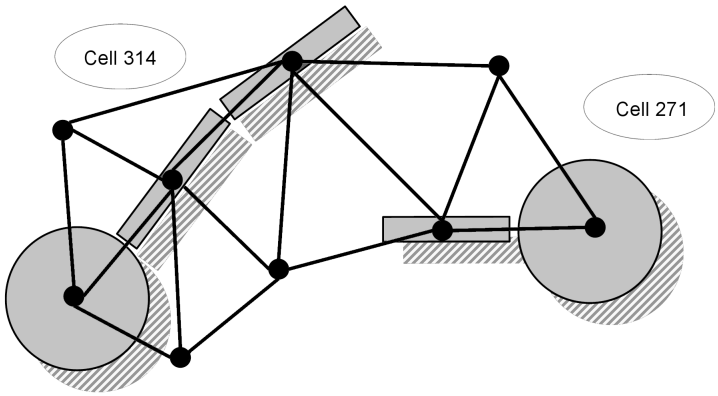

Figure 4.2: An illustration of how cells and space in CX3D are represented. Each object representing a part of a cell is present in the physical layer (grey with black edges) and the local biology layer (light grey stripes). Each has a unique label and a description of higher cellular processes in the cell layer (white ovals). The placement of nodes and vertices of the Delaunay triangulation are also shown (black balls and lines). The figure is adapted from the CX3D tutorial (Zubler, 2009).

one randomly determined side of the soma, and one apical dendrite on the side perpendicular to the basal dendrites. A single axon was initiated on the same side as the basal dendrites. In multipolar cells, 2-5 dendrites and one axon were initiated at random places on the soma.

Because in cultures axonal growth preceeds dendritic growth, the simulations were initialized with neurons that already have a small axon, between 9-11 μm in length. This compensates for the axons' initial growth before dendrites.

The elongation rate of the basal dendrites was set to a desired value, and the elongation rates of apical dendrites and axons were defined relative to that. The apical dendrites grew at a rate two times higher than the basal dendrites, and axons at a rate 4.5 times higher than the basal dendrites. These values are an approximate evaluation of the situation *in vitro*. The actual growth rates depend on many factors and can change over time, and thus are not straightforwardly measured accurately. The growth rate of apical dendrites was estimated from neuronal cell culture images in Kriegstein & Dichter, 1983. The growth rate of axons was chosen by comparing elongation rates of examples given in the NETMORPH manual (Koene et al., 2009a).

To test the simulators' capability to reproduce experimentallylly observed dendritic growth, the elongation rate parameter of the basal dendrites was varied. Values of 2, 6, 10, 14 and 22 μm/day were simulated. The elongation rates of apical dendrites were in these cases 4, 12, 20, 28 and 44 μm/day, and the elongation

rates of axons were 9, 27, 45, 63 and 99 μm/day, respectfully. Elongation rate of dendrites of multipolar cells is always the same as the elongation rate of basal dendrites of pyramidal cells. For these simulations, an attraction parameter that is present only in CX3D to define an attraction force between axons and soma, was set to 0. Simulation time step in NETMORPH was set to 1 hour and in CX3D to 0.1 hours. In CX3D the time step was set smaller, because the algorithm was unable to reproduce realistic morphologies of neurons with a larger time.

The synapse formation model is different in the simulators due to their differing intrinsic properties. In NETMORPH, synapse formation is defined by a probability function that is inversely proportional to the distance between an axon and a denrite. The parameter controlling the function is the maximal distance between a presynaptic and a postsynaptic site which can be considered as a candidate pair for synapse formation. These distances are listed in table 4.1. In CX3D the synapse formation takes the distance between an axon and a dendrite into account in a different way. A synapse can be formed when a dendritic spine and an axonal bouton, a primal structure for synapse formation, are oriented towards each other, and the distance between them is smaller than the average spine length plus the average bouton length. See table 4.1 for spine and bouton lengths.

4.3.2 Model 2: Testing a larger network with NETMORPH

To assess the effect of network size on network properties, a network of 1000 neurons was simulated. The simulation space was scaled to correspond to the same density of neurons as in Model 1, namely, 100 cells/mm^2. The percentages of pyramidal and multipolar cells were kept as 80% and 20%, respectfully. Also, all other parameters were the same as in the simulations of 100 cells. The number of cells was chosen to be 1000 because the simulations with NETMORPH were still not too heavy and time consuming, but the network was reasonably bigger than the previously simulated. With CX3D this test was impossible to conduct, because with considerably more than 100 neurons, the simulations became too memory consuming to be simulated in a reasonable time even on the server used for simulations. The basal dendrite elongation rate in this model was 2 μm/day. Elongation rates of apical dendrites and axons were 4 μm/day and 9 μm/day, respectfully. Elongation rate of dendrites of multipolar cells is always the same as the elongation rate of basal dendrites of pyramidal cells. All parameter values used in the simulations are listed in Table 4.1. Because of exceedingly heavy simulations, other growth rates were not tested.

4.3.3 Model 3: Testing short-range attraction with CX3D

To test an interesting feature in CX3D, a model mimicking short range attraction between axons and neuronal cell bodies was simulated. In this model, if an axon comes within a distance of 1 μm of a soma, the soma exerts an attracting force towards the axon. The force is determined by defining the parameter *axon_w*. This component is present only in CX3D, and we were interested to see if it could be used as a simple way of mimicking the effect of axon guidance cues. Biologically, a short range attraction of this type could result from interactions of the growth cone with the extracellular matrix immediately surrounding the soma, with surface proteins of the soma, or alternatively, due to the effects of a very short range diffusible guidance cue. Attraction parameter values 0, 2.5, 5, 10 and 20 were tested for comparison. The number of cells in this model is 100, and cell ell density and proportions of different types of neurons are the same as in the other two models. The basal dendrite elongation rate in this model was 10 μm/day. Elongation rates of apical dendrites and axons were 20 μm/day and 45 μm/day, respectfully. Elongation rate of dendrites of multipolar cells is always the same as the elongation rate of basal dendrites of pyramidal cells. All parameter values used in the simulations are listed in Table 4.1.

4.3.4 Parameter values used in the simulations

The parameter values chosen for the simulations are listed in table 4.1. The table contains a list of parameters in the model, values for the parameters, the model in which each parameter value was used, and a reference for the criteria the selection of the parameters is based on. The models indicated in table 4.1 are described in more detail in table 4.2, and the references for the choice of the particular parameter values are listed in table 4.3.

4.4 Methods for analyzing the simulated networks

4.4.1 Synapse count

Counting the number of synapses per neuron is a simple way of comparing the simulated networks. The synapse count can help in pointing out the differing behaviour of the different synapse formation models of CX3D and NETMORPH. For synapse count, all presynaptic and postsynaptic sites of each neuron are counted. synapses

	Parameter	*	Value	Unit	Reference
CELL	number of neurons	1,3	100		K
		2	1000		L
	pyramidal cells	1,2,3	80	%	G
	nonpyram. cells	1,2,3	20	%	G
	density of neurons	1,2,3	100	$\frac{cells}{mm^2}$	F,G,H,I,K
	soma diameter	1,2,3	10	μm	B
	attraction	1,2	0		M
		3	0, 2.5, 5, 10, 20		M
BASAL (APICAL) DENDRITE	ν_0	1	2, 6, 10, 14, 22	$\frac{\mu m}{day}$	C
		2,3	10	$\frac{\mu m}{day}$	C
		1,2,3	$(2 \times \nu_{0BASAL})$	$\frac{\mu m}{day}$	C,D
	F	1,2,3	0		C
	B_{inf}	1,2,3	2.52		C
	τ	1,2,3	3.006	$days$	C
	E	1,2,3	0.73		C
	S	1,2,3	0.5		C
NON-PYRAMIDAL DENDRITE	ν_0	1,2,3	ν_{0BASAL}	$\frac{\mu m}{day}$	C,E
	F	1,2,3	0		C,E
	B_{inf}	1,2,3	2.6475		C,E
	τ	1,2,3	4.706	$days$	C,E
	E	1,2,3	0.594		C,E
	S	1,2,3	-0.259		C,E
AXON	ν_0	1,2,3	$4.5 \times \nu_{0BASAL}$	$\frac{\mu m}{day}$	C
	F	1,2,3	0.16		C
	B_{inf}	1,2,3	17.38		C
	τ	1,2,3	14	$days$	C
	E	1,2,3	0.39		C
	S	1,2,3	0		C
SYNAPSES: NETMORPH	distance pyr.-pyr.	1,2	1	μm	C
	distance pyr.-nonpyr.	1,2	0.1	μm	C
	distance nonpyr.-pyr.	1,2	1	μm	C
	distance nonpyr.-nonpyr.	1,2	0.1	μm	C
SYNAPSES: CX3D	spine length	1,3	3	μm	A,J
	bouton length	1,3	2	μm	J

Table 4.1: Parameters used in the simulations. Left column: the part of the model the parameter affects. Parameter: name of the parameter. *: the model in which the parameter value was used. See table 4.2 for explanation. Value: numerical value of the parameter. Unit: unit of the value. Reference: references to the literature the choice of parameter value was based on. See table 4.3 for explanation.

	Model	Simulator
***1**	Model 1: Comparing the simulators	NETMORPH, CX3D
***2**	Model 2: Testing a larger network	NETMORPH
***3**	Model 3: Testing the effects of short-range attraction	CX3D

Table 4.2: Models indicated in the column * of table 4.1. See section 4.3 for a more detailed description about the models, and section 4.2 for a description of the simulation tools.

	Reference for selection of parameter value
A	Hering & Sheng, 2001
B	Ichikawa et al., 1993
C	Koene et al., 2009b
D	Kriegstein & Dichter, 1983
E	de Lima & Voigt, 1997
F	de Lima & Voigt, 1999
G	Marom & Shahaf, 2002
H	Nakanishi & Kukita, 1998
I	Wagenaar et al., 2006
J	Zubler & Douglas, 2009
K	Limitations of either simulator
L	Testing effect of network size
M	Testing effect of varying attraction

Table 4.3: References for the selection of the parameter values listed in table 4.1, column "Reference".

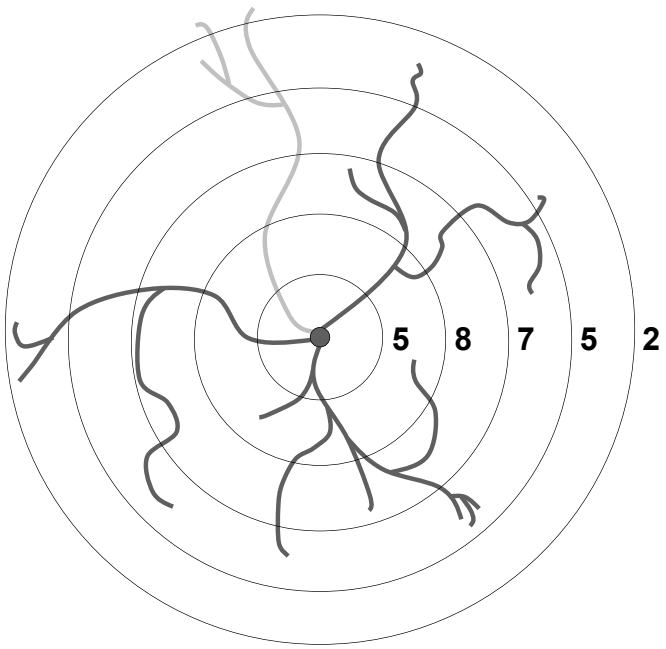

Figure 4.3: Sholl analysis. Crossings of neurites with each concentric circle are counted. The counts have been marked on the right side of each circle. Axon (light gray) and dendrites (dark grey) can be analysed separately, if wished. This method is technically possible to use in young neuronal cell cultures that are not yet completely covered in a dense network of neurites.

can also be counted in *in vitro* experiments (see *e.g.* Ichikawa et al., 1993), providing a way to compare simulation results with biological experiments.

4.4.2 Sholl analysis

Sholl analysis is a way of estimating the spatial extent of a dendritic tree (Uylings & van Pelt, 2002). For the analysis, a set of equidistant concentric circles is placed around the soma of the neuron, and the number of dendrites and axons crossing each circle is counted. This method can be used by biologists because of it's technical easiness and ability to detect large differences in dendritic branching between different cells. However, this method is not very sensitive, since it does not discriminate between different types of dendritic trees, or differences in dendritic orientations. In this work, it is used to evaluate the overall dendritic morphology in the simulated cultures.

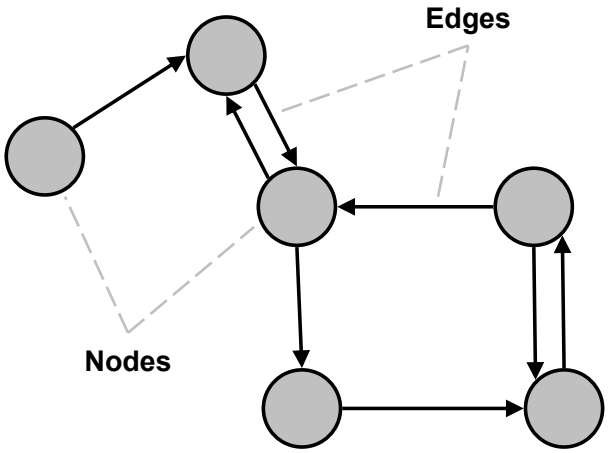

Figure 4.4: Graph representation of a network of neurons. In the representation, neurons are marked as nodes, denoted by the circles. The synaptic connections between neurons are marked as directed edges, denoted by the arrows that point towards the postsynaptic cell. Two examples of nodes and edges have been pointed out in the figure.

4.4.3 Graph representation of neuronal networks

One way to analyze the structure of neuronal networks is to reduce them to graphs (Newman, 2003). In a graph representation, only neurons and the synaptic connections between them are considered. Morphology of the cells and their axons and dendrites, and their embedding in space, are not taken into account. In a graphical representation, each cell is called a "node" in the network. If a synaptic connection exists between two cells, an "edge" is drawn between them to represent a connection. These connections are always directed, because the only allowed direction of propagation of action potentials is from the axon of one cell to the dendrites of another. Thus the directionality of an edge is represented by an arrowhead pointing towards the postsynaptic cell. If the number of synapses between two cells is to be taken into account, the thickness or "weight" of an edge can be varied according to the number of synapses existing between the axon of the presynaptic cell and the dendrites of the postsynaptic cell. The graph is then called a weighted graph. Only unweighted graphs are used in the analysis of results in this work. Figure 4.4 shows an example of graph representation of a network of neurons.

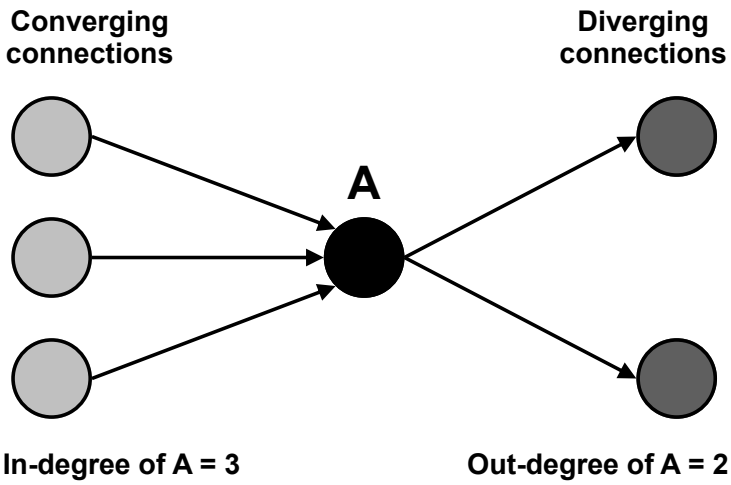

Figure 4.5: In-degree and out-degree of a cell. The axons of the cells on the left are synaptically connected to the dendrites of cell A. These cells add up to the number of in-degree of cell A. The axons of cell A are synaptically connected to the dendrites of the cells on the right. These cells add up to the number of out-degree of cell A.

4.4.4 In-degree and out-degree

In-degree and out-degree are parameters describing the incoming (converging) and outgoing (diverging) connections of a cell, respectively (Newman, 2003). In-degree is the number of incoming connections. For a neuron, this would mean axons of other cells connecting with the neuron. Out-degree is the number of outgoing connection. For a neuron, this is the number of othe neurons the cell is connected to with its axons. Mean in-degree and out-degree over a whole network describe the average connectivity of individual neurons to other neurons. From a graph representation, the in-degree of a node is computed by counting the directed edges arriving to a node, and the out-degree by counting the edges leaving from the node. See figure 4.5 for an illustration of defining in-degree and out-degree.

4.4.5 Shortest path length

The shortest path between two nodes is the route that passes through the least amount of edges while getting from the starting node to the ending node (Newman, 2003). Edges can be passed only in the direction of the arrow, not against it. In a neuronal culture, the shortest path measure would represent the route with the least synaptic clefts to cross for an action potential to travel from the starting point of the action potential, to the "end point" neuron receiving it. Figure 4.6 shows a simple example of counting the shortest path.

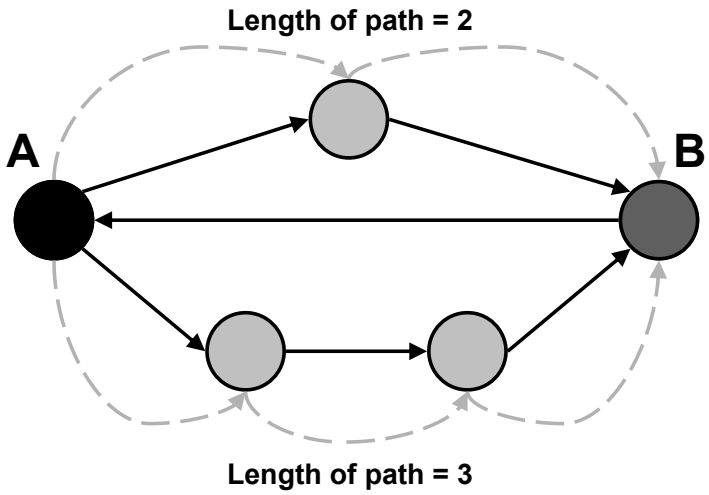

Figure 4.6: Calculating the shortest path from cell A to cell B. Paths from A to B are marked with grey dash line arrows. The upper path has two edges, and the lower one has three. Thus the upper path is the shortest path between cells A and B.The direct connection between A and B (in the middle) can not taken into account, because it is in the wrong direction (from presynaptic cell B to postsynaptic cell A).

4.4.6 Motifs

One way of analyzing the structure of a complex network is to count the number of different motifs that appear in the network (Milo et al., 2002). Motifs are different patterns of connectivity between nodes. In this work, connectivity motifs between three neurons are analyzed. All connected triplets of neurons are classified into one of the thirteen possible types motifs according to the cells' mutual connections (see figure 4.7). Motifs can be considered as tiny circuits within the larger circuitry of the neuronal network. Quantitative analysis of the motifs apperaring in a network is a way to classify the structure of the obtained network (Milo et al., 2002; Newman, 2003). Different types of networks, such as gene regulatory networks, neuronal networks, food chain networks or the world wide web, have been shown to have a different motif composition (Milo et al., 2002).

4.4.7 Simulation environments

Two servers will be used for performing the simulations. Both are running 64 bit GNU/Linux. The first one has 8 4-core Intel Xeon E5420 2,50 GHz processors and 33 GB of memory, and the second one has 24 6-core 2,66 MHz Intel Xeon X5650 processors and 62 GB of memory.

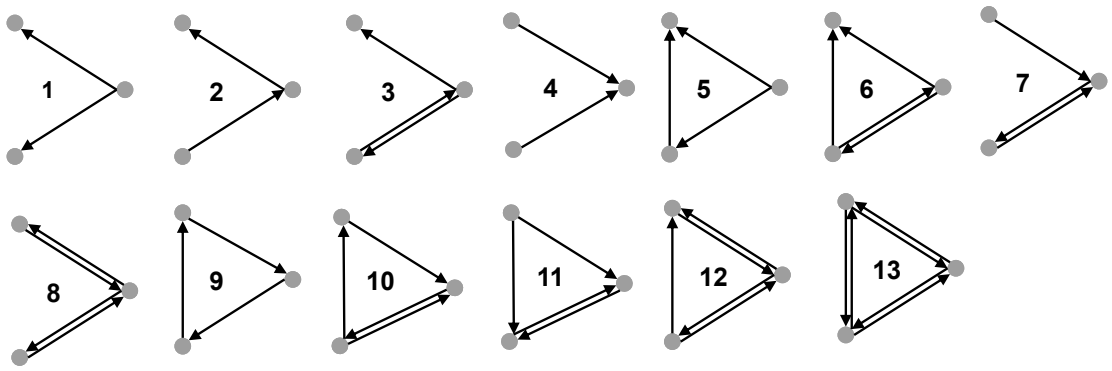

Figure 4.7: Graph representation of the 13 different motifs of connectivity between a triplet of cells.

5 Results

In total, three models were built and simulated. Model 1 was simulated 50 times with CX3D and 119 times with NETMORPH. These simulations will be referred to as CX3D1 and NETMORPH1, respectively. Model 2 was simulated 20 times with NETMORPH. These simulations are referred to as NETMORPH2. Model 3 was simulated 49 times with CX3D, and these simulations are referred to as CX3D3. The CX3D simulations took time in the scale of tens of minutes per simulation, depending on the growth rates of neurites. Bigger growth rates resulted in heavier simulations. The NETMORPH simulations for a network of 100 cells took some minutes per simulation, and for a network of 1000 cells tens of minutes, with the basal dendrite growth rate 2 μm/day. For the 1000 cell network, growth rates larger than this tended to make the simulations very heavy, and with the basal dendrite growth rate 10 μm/day, the set of 20 simulations would have taken about two weeks on the faster of the two used servers. Thus only the basal dendrite growth rate 2 μm/day was used for the network of 1000 cells.

The growth rates used in the simulation are expressed through declaring the basal dendrite growth rate of pyramidal dendrites in the simulations. Growth rates of other neurites always scale relative to this. For pyramidal neurons, the apical dendrite growth rate is two times that of the basal dendrite growth rate, and for multipolar neurons, the growth rate of all dendrites is the same as the basal dendrite growth rate of pyramidal neurons. Axons of neurons grow at a rate 4,5 times higher than the basal dendrite growth rate of pyramidal neurons.

For all the tested parameters, Model 3 produced practically exactly the same results as Model 1 in CX3D with a growth rate of 10 μm/day. This suggests that varying the attraction parameter did not affect the properties of the produced networks. The reasons behind this result will be discussed further in section 6.3.3. Model 3 result figures are presented in the current section, but not commented separately.

Parts of the results presented here are published in Aćimović et al., 2011 and Mäki-Marttunen et al., 2010.

5.1 Analysis of simulated neuronal features

5.1.1 Synapse count

The number of synapses per neuron varies expectedly with the growth rate of the neurites, bigger growth rates leading to larger numbers of synapses. Figure 5.1 shows the evolving of number of synapses per neuron in the simulated neuronal networks. The x axis in the figure represents the deevelopment time in days, and the y axis represents the number of synapses per neuron. For models NETMORPH1, CX3D1 and NETMORPH2, the different colors of curves denote the simulations with different growth rates of neurites. The growth rate is expressed as the basal dendrite growth rate, and the growth rates of other dendrites scale relative to that. Apical dendrites grow at a rate two times faster than the basal dendrites, and axons of all neurons at a rate 4,5 times faster than the basal dendrites. All dendrites of multipolar neurons grow at the rate of basal dendrites of pyramidal neurons. For model CX3D3, the different colors represent the different values for the attraction parameter. For this model, the basal dendrite growth rate is 10 μm/day. Bars represent the standard deviation at each time point.

In their previous studies, Ichikawa et al., 1993 have calculated the number of synapses per cell simply by counting the synapses in the culture, and dividing this number by the number of cells (Ichikawa et al., 1993). Thus each synapse has been counted to be part of only one cell. In the case of our simulation results, however, the synapse count per neuron is a sum of all the neuron's postsynaptic sites, and all its presynaptic sites. This means that each synapse is counted twice, once for its presynaptic cell, and once for its postsynaptic cell. To enable comparison of our results to the results of Ichikawa et al., 1993, the experimentally observed values of numbers of synapses per neuron stated in Ichikawa et al., 1993 are multiplied by two. These twofold values are marked in the figures with *.

Model 1. In CX3D, the basal dendrite growth rates larger than 10 μm/day tend to produce more synapses per neuron, and the ones smaller than 10 μm/day less synapses per neuron than what has been experimentally observed. Bigger growth rates systematically produce bigger numbers of synapses per neuron in both simulators. The rate of synapse formation with a basal dendrite growth rate of 10 μm/day agrees quite well with the observed experimental synapse numbers with the same estimated growth rate, until 14 DIV in the simulation (Ichikawa et al., 1993). After that, CX3D overproduces synapses compared to experimental observations, and at 21 DIV the growth rate that agrees the best with experimentally observed

numbers of synapses is 6 μm/day. NETMORPH, however, produces a very large amounts of synapses from the beginning, and with the growth rates of 6 and 10 μm/day the number of synapses greatly exceeds the experimentally observed number. At 21 DIV, the growth rate 2 μm/day produces a synapse number very close to the experimentally observed one. These results are shown in figure 5.1, two upper panels.

Model 2. Compared to a network of 100 cells, by 21 DIV the network of 1000 cells with a basal dendrite growth rate of 2 μm/day produces a bit more than twofold number of synapses compared to the network of 100 cells with the same growth rate. The reason for this is the larger total amount of cells in the model. The shape of the synapse count growth curve is similar to that of the 100 cell network with the same growth rate. These results are presented in figure 5.1, lower left panel.

5.1.2 Sholl analysis

Sholl analysis was performed for neurons of Model 1 simulated in both CX3D and NETMORPH with a growth rate of 10 μm/day for basal dendrites (20 μm/day for apical dendrites and 45 μm/day for axons), to compare the neuronal morphology the simulation tools produce. The x axis of the Sholl analysis histograms represents Sholl circle radius (distance from the cell soma), and the y axis represents the mean number of crossings of neurites with each circle. The histogram colors indicate the simulation day for which the Sholl analysis was performed.

The Sholl analysis histograms for neuronal networks simulated with both simulation tools, and for all analyzed types of neurites, acquire a higher and wider shape with passing simulation time. This shows that the neurites are getting longer and they are branching more with time. The peak height of the curve represents the distance from the cell soma where the largest mass of neuritic branches is situated. Comparison of Sholl analysis between the two simulation tools reveals a difference in the morphology of neurons between NETMORPH and CX3D. The neurites in NETMORPH branch twice as much as the ones in CX3D, and also grow longer. The general shape of the Sholl analysis histograms is still similar, showing that the overall morphology in neurons simulated with both tools is similar.

Sholl analysis of dendrites shows that the characteristic shape produced with both simulation tools is similar, although NETMORPH produces longer dendrites. Sholl analysis of dendrites produces in both tools a histogram that starts with a somewhat bell-like shape that is cut from the left end, and is followed by a longer tail (figure 5.2, two upper panels). The tail represents a group of dendrites that are longer than the

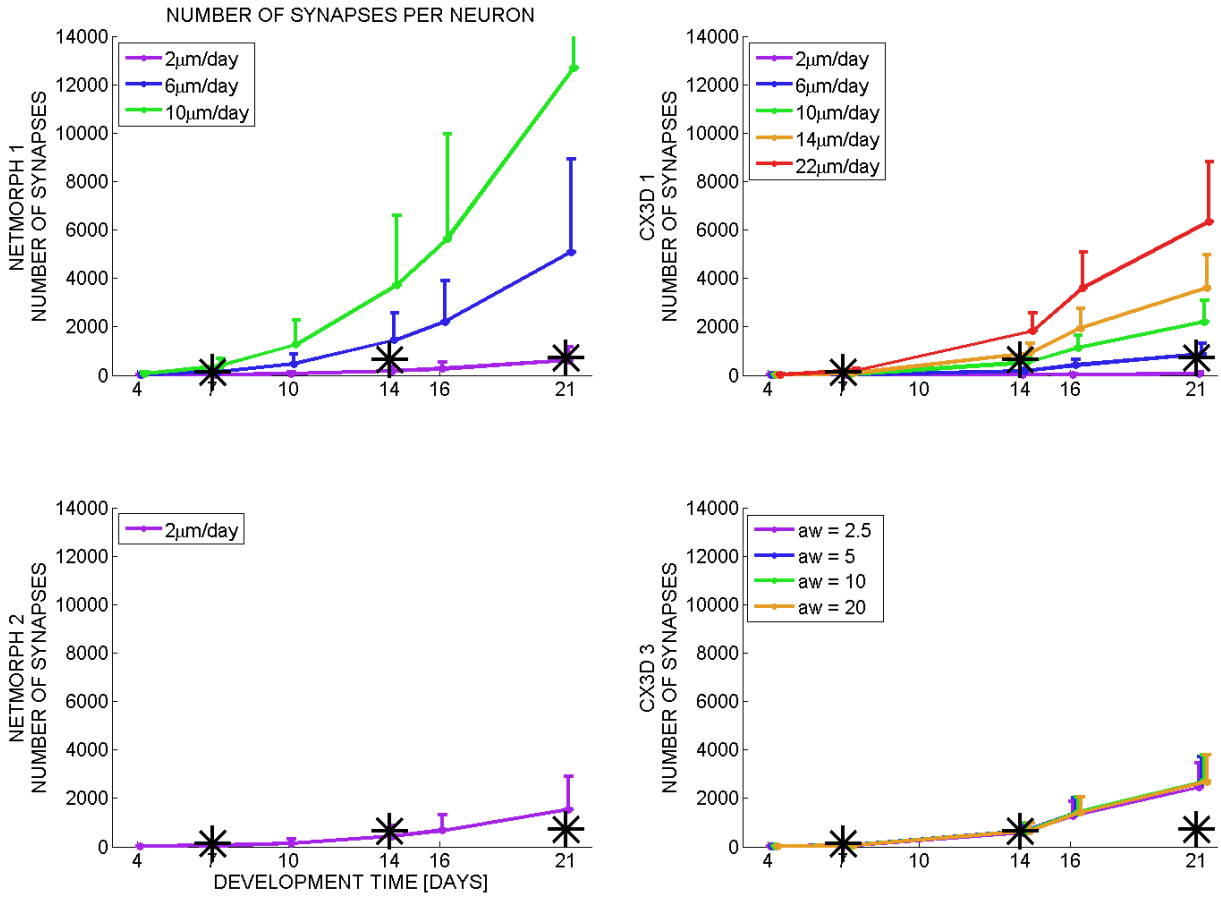

Figure 5.1: Number of synapses in the simulated neuronal networks. Top left panel: NETMORPH1. Top right panel: CX3D1. Bottom left panel: NETMORPH2. Bottom right panel: CX3D3. The x axis represents the days in culture, and the y axis represents the number of synapses per neuron. * marks the experimentally observed values for number of synapses per neuron on different days *in vitro*. For NETMORPH1, CX3D1 and NETMORPH2, the different colors of curves denote the simulations with different growth rates of neurites. The growth rate is expressed as the basal dendrite growth rate, and the growth rates of other dendrites scale relative to that. Apical dendrites grow at a rate two times faster than the basal dendrites, and axons of all neurons at a rate 4,5 times faster than the basal dendrites. All dendrites of multipolar neurons grow at the rate of basal dendrites of pyramidal neurons. For CX3D3, the different colors represent the different values for the attraction parameter. For this model, the basal dendrite growth rate is 10 μm/day. Bars represent the standard deviation at each time point.

general population of dendrites. As the simulation time proceeds, the height of the histograms rises steadily, showing the build-up of the number of dendritic branches. The histograms get wider and their tails longer, indicating that the dendrites gain length. With NETMORPH simulations, the dendrites start with a peak mass of 10 crossings at around 40 μm distance from the soma, and the longer "tail" dendrites reach about 100 μm distance at 4 DIV. The dendrites develop to have a peak mass of about 20 crossings at around 80-180 μm distance from the soma, and the "tail" dendrites reach 400 μm at 21 DIV. For CX3D simulations, these numbers are peak mass of 7 crossings at around 40 μm distance from the soma, and "tail" reaching nearly 100 μm at 4 DIV, and a peak mass of 10 crossings around 60 μm distance from the soma, and "tail" reaching a bit over 300 μm at 21 DIV.

Conversely to the case with dendrites, CX3D seems to produce a bit longer axons than NETMORPH. NETMORPH axons, on the other hand, tend to branch more. The Sholl analysis for axons in both simulation tools produces histograms that have a bell-like shape leaning towards right, indicating that the larger mass of axonal branches tends to lie in the farther end of the axonal tree (figure 5.2, two lower panels). The histograms steadily gain height and width as simulation time proceeds. The NETMORPH axons start with a peak mass of about 5 crossings around the distance 110 μm from the soma, and reach a maximum distance of a bit less than 200 μm at 4 DIV. They grow to to have a peak mass of almost 40 crossings at 300 μm distance from the soma, and a maximum distance of a bit more than 500 μm. CX3D axons start with a peak mass of 3 crossings at 110 μm distance from the soma, and a maximum distance of about 150 μm at 4 DIV. They grow up to have a peak mass of about 12 crossings at a distance around 220 μm and a maximum distance of about 600 μm at 21 DIV.

A separate Sholl analysis of dendrites of pyramidal cells shows that NETMORPH produces more branches and longer dendrites, based on the look of the histogram for pyramidal neuron dendrites (figure 5.3, two upper panels). In histograms of pyramidal dendrites of NETMORPH, for all analyzed days except 4 DIV, there is a visible "bump" followed by tail, which gets longer as simulation time proceeds. With pyramidal dendrites simulated with CX3D, the "bump" is clearly separate from the tail on 4 and 7 DIV, but the separation of these two becomes less clear on 14 and 21 DIV. With NETMORPH pyramidal dendrites, the dendrites start with a peak massof a bit more than 10 crossings at 10 μm distance from the soma, and maximum distance of about 100 μm at 4 DIV. The grow to have a peak of 20 crossings around 100-140 μm distance and a maximum distance of 400 μm at 21 DIV. Pyramidal dendrites from CX3D start with a peak mass of about 7 crossings around 30 μm

distance from the soma, and the tail reaching 100 μm at 4 DIV. They end up having a peak mass of about 11 crossings at a 50 μm distance and a maximum distance of about 300 μm at 21 DIV.

Sholl analysis of multipolar neurons' dendrites reveals that with both simulation tools, the shape of the multipolar dendrites' Sholl analysis histogram is always similar to the shape of the "bump" of a corresponding histogram of pyramidal dendrites, on the same simulation day and simulation tool (figure 5.3, two lower panels). The peaks masses of the dendrites on 4 and 21 DIV also correspond to the ones of pyramidal dendrites with both simulation tools, but the maximum reach of the dendrites is different. For NETMORPH, the maximum distance the multipolar neurons' dendrites reach is a bit less than 100 μm distance from the soma at 4 DIV, and about 250 μm at 21 DIV. For CX3D, the maximum reach at 4 DIV is 50 μm, and at 21 DIV it is a bit less than 200 μm.

Figure 5.4 shows examples of Sholl analysis of the whole culture for one example culture with both NETMORPH and CX3D 14 DIV. The x axis represents individual neurons, numbered from 1 to 100. The y axis represents the distance from the cell soma, starting from 0 μm in the upper part and growing downwards. The number of neurites crossing each Scholl circle (the Sholl measure) is color coded. Colors in the blue end of the spectrum represent smaller numbers of crossings, and colors in the red end of the spectrum represent a larger number of crossings. It can bee seen from the brighter colors and bigger reach of the colors that in NETMORPH, both axons and dendrites tend to exhibit more extensive branching and greater length than in CX3D. The Sholl analysis of dendrites is shown in the two upper panels of figure 5.4, and the Sholl analysis axons in the two lower panels.

Anomalies observed through Sholl analysis. Sholl analysis of individual neurons simulated CX3D sometimes shows a sudden, remarkable increase in the number of neurites crossing a Sholl circle. These exceptions are evened out in the statistical analysis of the results. A closer inspection of the Sholl analysis of such a neuron reveals that indeed, a sudden, up to four-fold increase in the number of crossings of axons or dendrites takes place within an interval of a few tens of micrometers. The number of crossings will also immediately drop back to the original range when distance from soma further increases. This kind of observations are not made with NETMORPH simulations.

An example of such a case is shown in Figures 5.3 and 5.6. It seems very unlikely that neurites would suddenly create a large amount of new branche in the simulations. In such case these new arbors would continue to grow as defined by the model, gaining

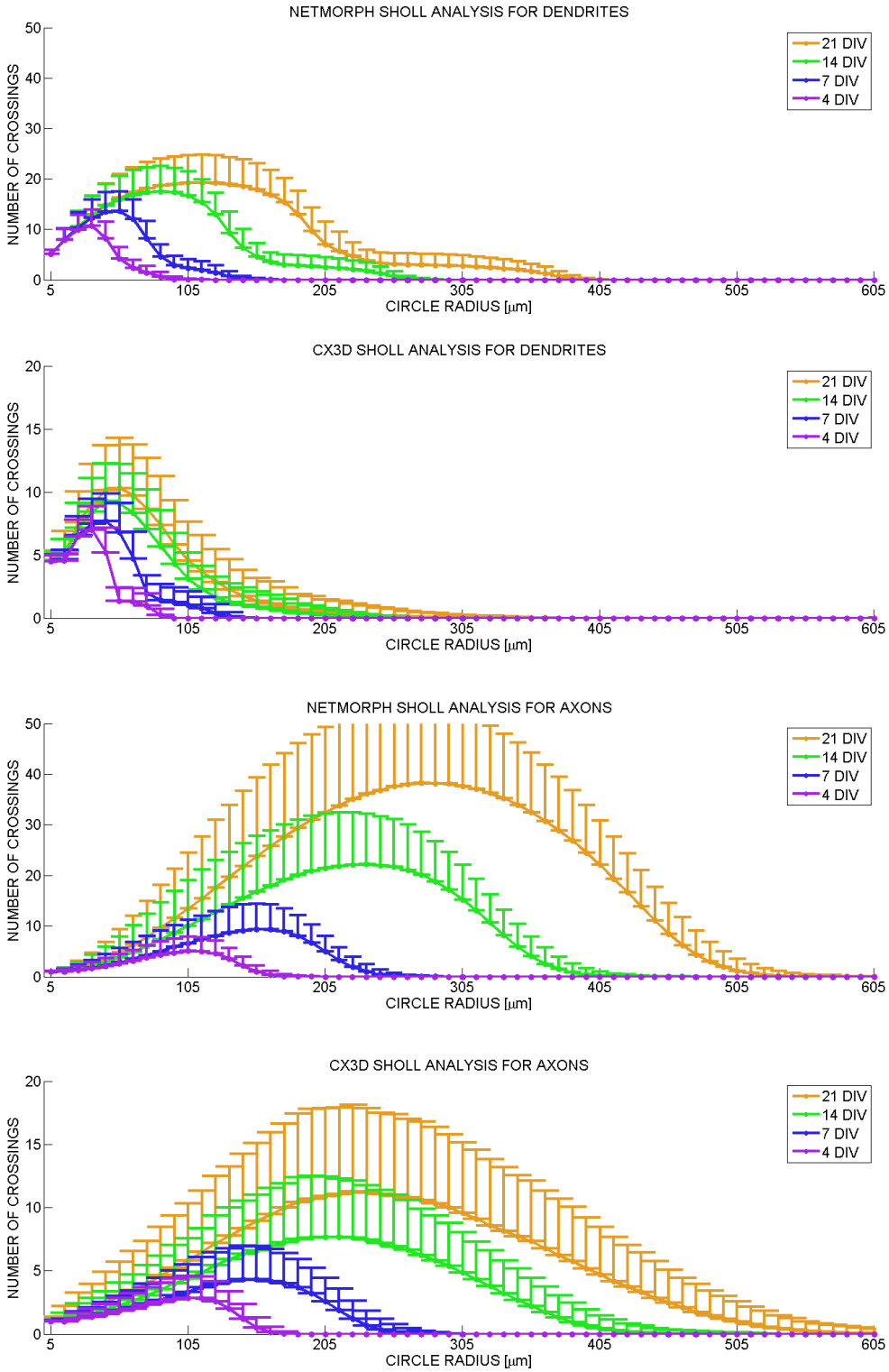

Figure 5.2: Sholl analysis for axons and dendrites of neurons simulated with NETMORPH and CX3D. The growth rate of 10 μm/day for basal dendrites, 25 μm/day for apical dendrites and 40 μm/day for axons. The panels from up downwards: Sholl analysis for NETMORPH dendrites, Sholl analysis for CX3D dendrites, Sholl analysis for NETMORPH axons, Sholl analysis for CX3D axons. The x axis represents the distance from cell soma, and y axis represents the number of neurites crossing each Sholl radius. The different colors represent the analyzed simulation days. The bars represent the standard deviation at each point.

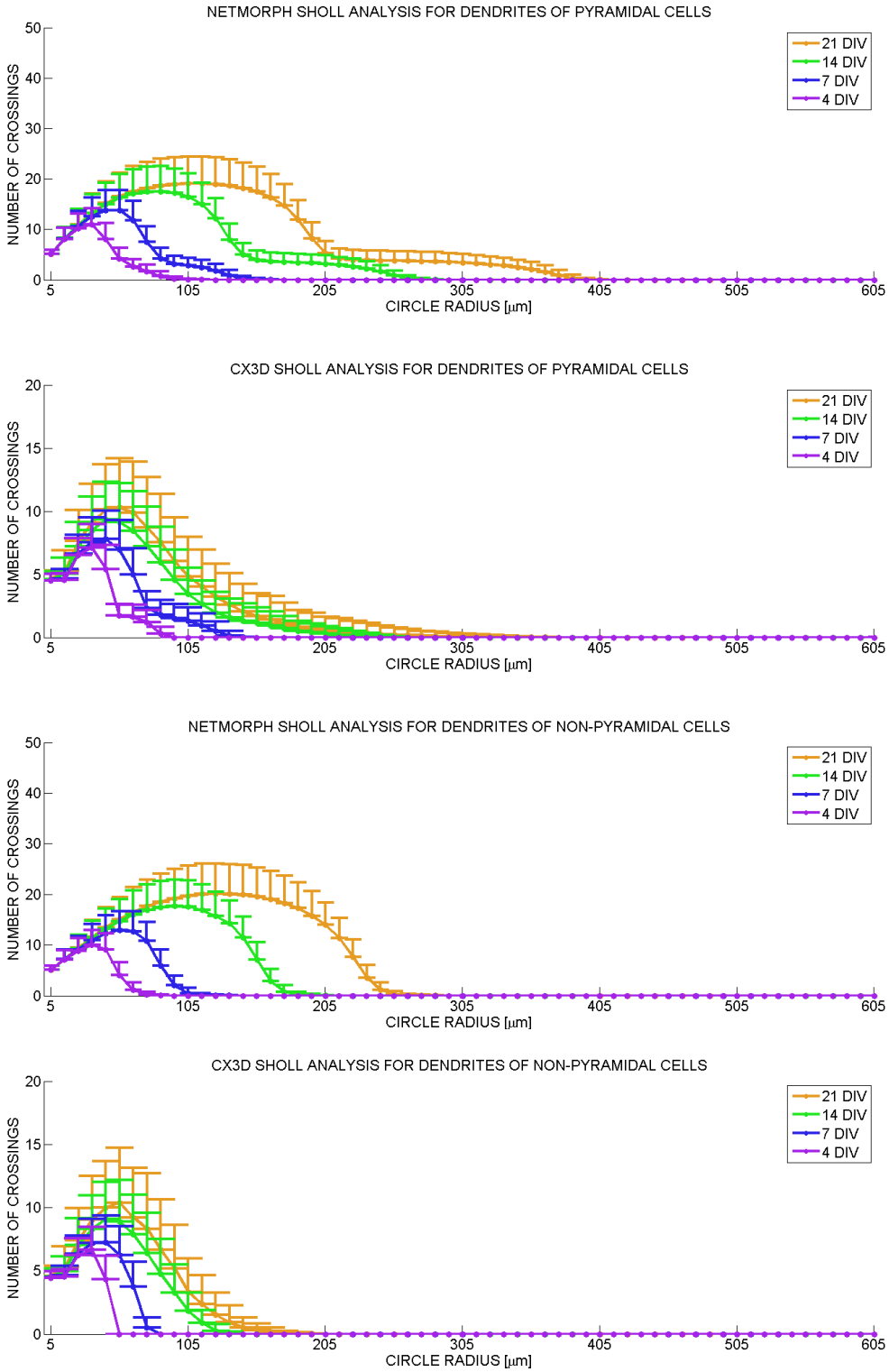

Figure 5.3: Sholl analysis for dendrites of pyramidal and multipolar neurons simulated with NETMORPH and CX3D. The growth rate of 10 μm/day for basal dendrites, 25 μm/day for apical dendrites and 40 μm/day for axons. The panels from up downwards: Sholl analysis for NETMORPH pyramidal cell dendrites, Sholl analysis for CX3D pyramidal cell dendrites, Sholl analysis for NETMORPH multipolar cell dendrites, Sholl analysis for CX3D multipolar cell. The x axis represents the distance from cell soma, and y axis represents the number of neurites crossing each Sholl radius. The different colors represent the analyzed simulation days. The bars represent the standard deviation at each point.

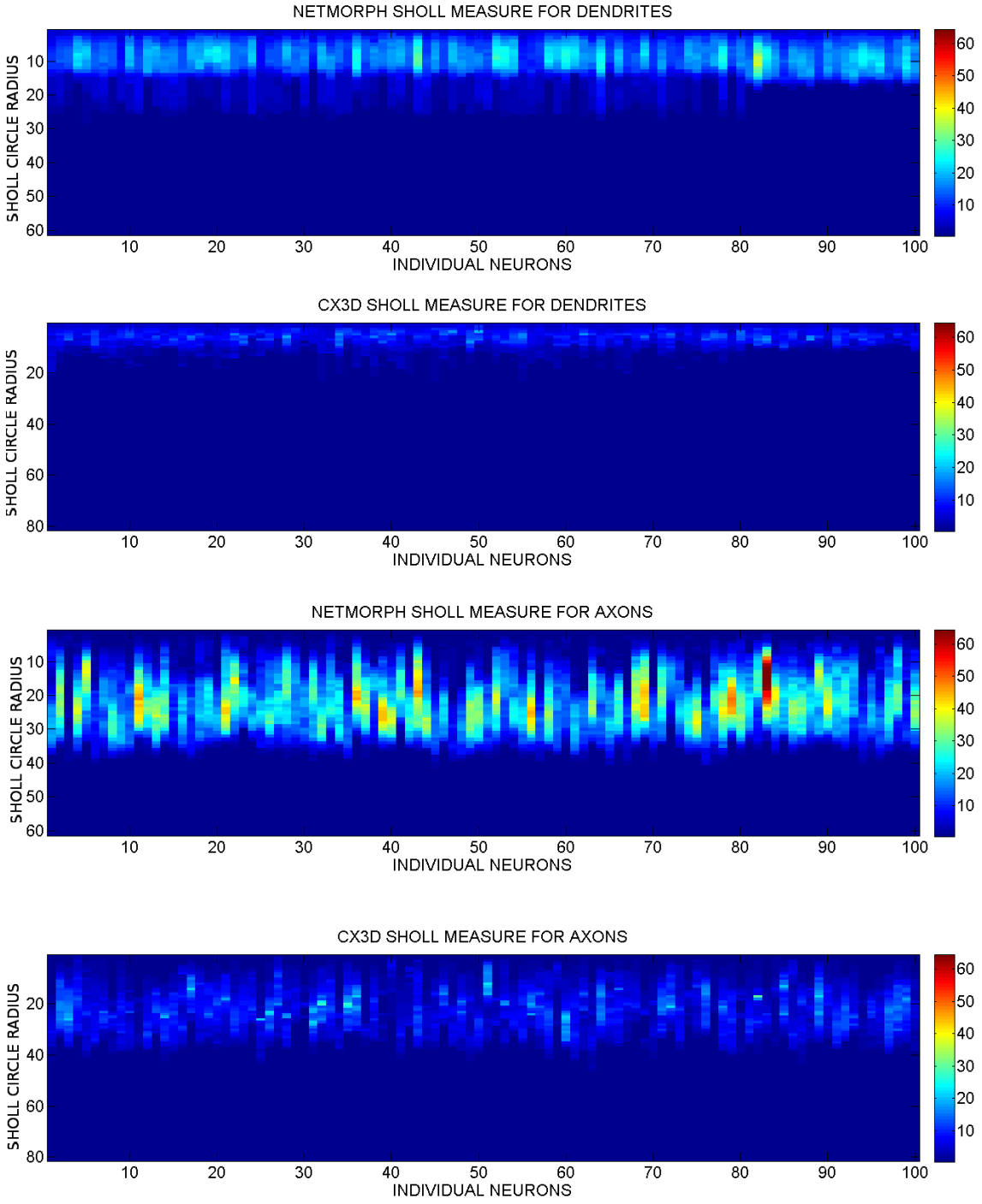

Figure 5.4: Examples of Sholl analysis of one simulation.The panels from up downwards: Sholl analysis for NETMORPH dendrites, Sholl analysis for CX3D dendrites, Sholl analysis for NETMORPH axons, Sholl analysis for CX3D axons. All figures are from day 14 of an arbitrarily chosen simulation. The x axis represents individual neurons, numbered from 1 to 100. The y axis represents the distance from the cell soma, starting from 0 μm in the upper part and growing downwards. The number of neurites crossing each Scholl circle (the Sholl measure) is color coded. Colors in the blue end of the spectrum represent smaller numbers of crossings, and colors in the red end of the spectrum represent a larger number of crossings.

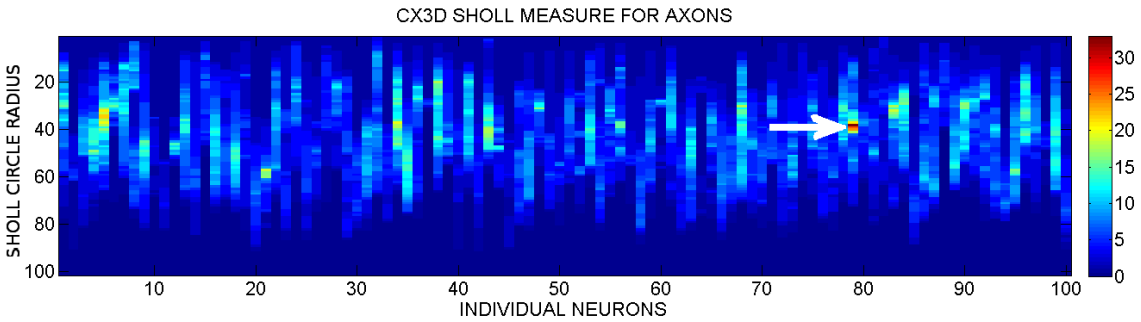

Figure 5.5: Sholl analysis of axons in one CX3D simulation at 14 DIV. The x axis represents individual neurons, numbered from 1 to 100. The y axis represents the distance from the cell soma, starting from 0 μm in the upper part and growing downwards. The number of neurites crossing each Scholl circle (the Sholl measure) is color coded. Colors in the blue end of the spectrum represent smaller numbers of crossings, and colors in the red end of the spectrum represent a larger number of crossings. The arrow is showing a suspiciously high number of crossing axons appearing suddenly and disappearing quickly.

length, and eventually crossing more and more Sholl circles. This cannot have been the case in Figure 5.6, since the arbors suddenly appear in the middle of the neuritic trees, but do not seem have grown more than some tens of micrometers.

When the neuritic arbors of this kind are visualized, they show a tightly packed zig-zag formation in a neurite at the exact distance from the soma indicated by the sudden increase of neurites crossing a Sholl circle. These zig-zags cause the same neurite to jump back and forth over the same Sholl radius line several times. The four-fold increase of crossings in figure 5.6 is actually caused by two separate zig-zags in different branches of the axonal arbor, coincidently crossing consecutive Sholl radius circles. This is seen in figure 5.7. The zig-zags are formed when CX3D exerts a force towards a neurite growing strongly "up" or "down" , reaching the z dimension boundary of the simulation space. The force pushes the neurite towards the other z dimension boundary, and the same happens several times in a row. This could be avoided by limiting the growth directions of the neurites.

5.2 Analysis of network structure

5.2.1 In-degree

The mean in-degree was computed for the networks simulated with both tools. In the in-degree analysis figures 5.8, the x axis represents the mean in-degree, and y axis represents the mean percentage of cells having a particular in-degree. In the three uppermost rows, the curve colors indicate the basal dendrite growth rate used

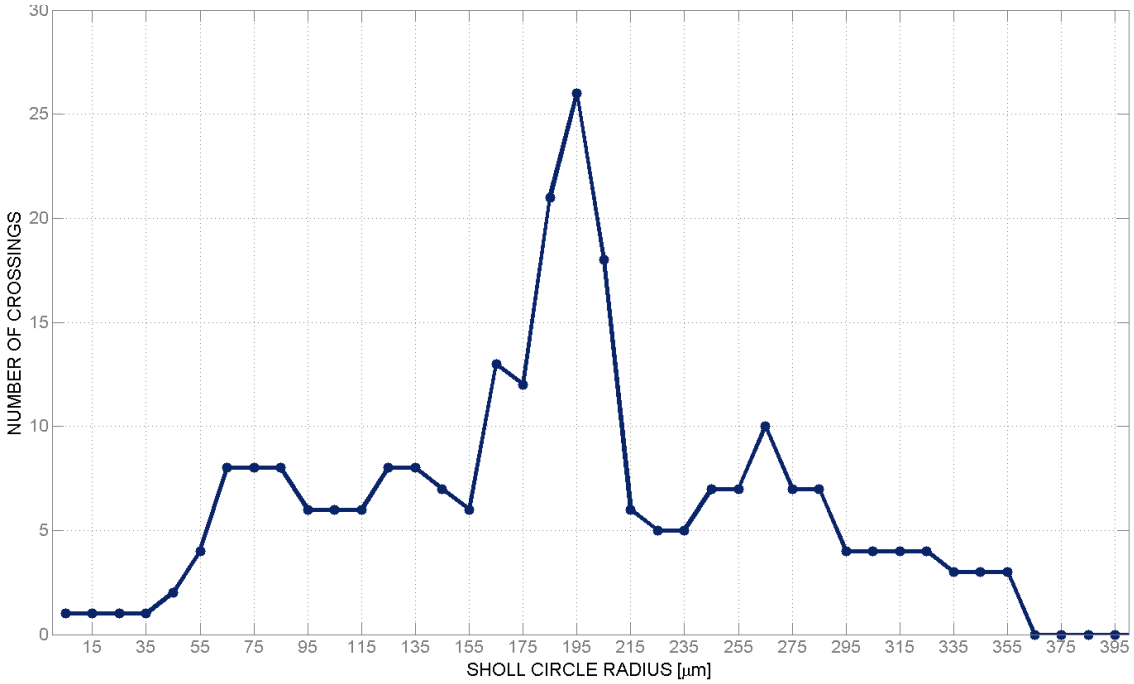

Figure 5.6: Sholl analysis of an individual neuron's axonal arbor at 14 DIV, simulated in CX3D. This is the neuron pointed out by the arrow in figure 5.5. The analysis shows a sudden increase and the following drop of the branches of the neuron's axon crossing the sholl radii between 155 μm and 215 μm distance from the soma of the cell. The x axis represents the distance from the cell soma, and the y axis represents the number axonal branches crossing each Sholl radius.

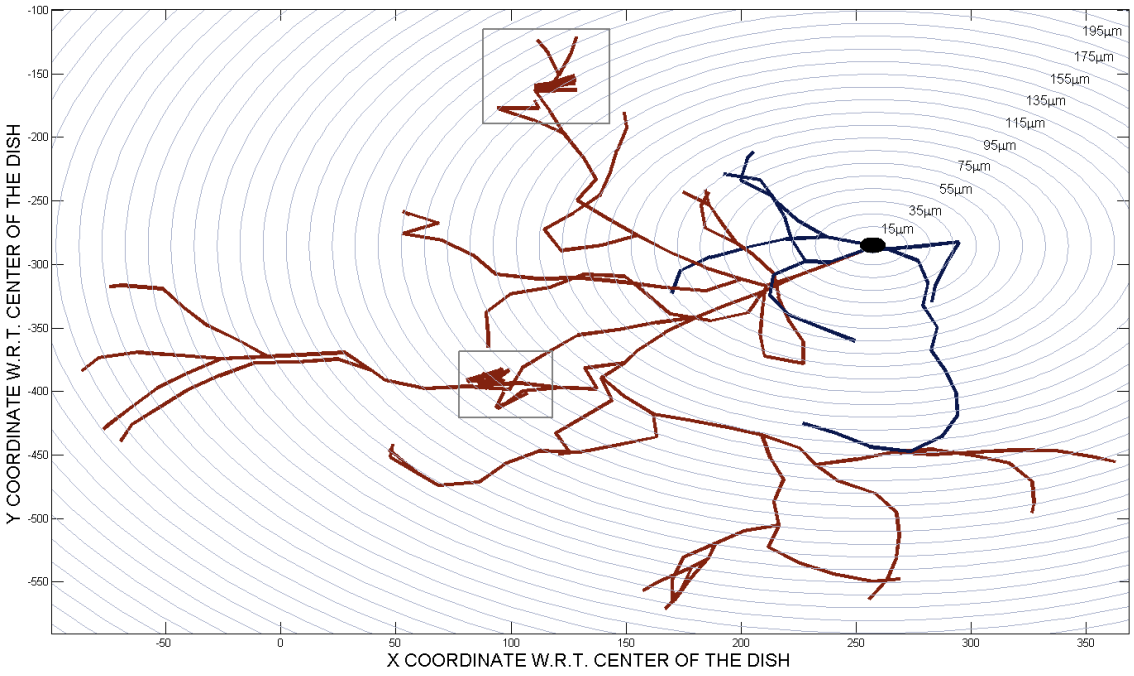

Figure 5.7: A visualization of the dendritic and axonal arbor of a neuron with zig-zags. This is the neuron pointed out by the arrow in figure 5.5, and analyzed in figure 5.6. The x axis represents the x coordinate with respect to the center of the dish, and the y axis represents the y coordinate with respect to the center of the dish. Distances of the Sholl radius circles form the cell soma are shown below the corresponging circle on the upper right side of the image. The cell soma is represented as a black circle, dendrites as dark blue lines, and the axon as red lines. The two zig-zag areas have been marked with boxes. These are the areas causing the sudden increase in axons crossing the Sholl radius circles shown in figures 5.5 and 5.6.

in the simulation. Growth rates of other neurites scale according to this, apical dendrites having a growth rate two times faster than the basal dendrites, and axons of all neurons 4,5 times faster than the basal dendrites. All dendrites of multipolar neurons grow at the rate of basal dendrites of pyramidal neurons. In the lowest row, the curve colors indicate the attraction parameter values.

Model 1. The mean in-degree was computed for networks simulated with Model 1 with different growth rate parameter values and both simulation tools. The results are shown in figure 5.8, two upper rows. The in-degree distribution obtains a more spread-out shape and a peak occurring at larger in-degree values, the bigger the growth rate is and the longer the network is simulated. This shows that the number of incoming connections per cell increases with passing simulation time, and the range of in-degrees different cells have also increases. With all simulated growth rates, NETMORPH produced a wider distribution of in-degrees than CX3D with the same basal dendrite growth rate, and about twice higher maximum in-degree than CX3D.

The mean in-degree of any given simulation day depends strongly on the growth rates of neurites. With NETMORPH (figure 5.8, first row), with a basal dendrite growth rate 2 μm/day, the in-degree distribution starts from a peak at the in-degree numbers nearing zero (more than 40 % of neurons) at 4 DIV, and the maximum in-degree is less than 5. This means that the neurons have few connections, if any, at this point. At the same time point, the basal dendrite growth rate 10μm/day produces a peak at in-degree of about 5 (20 % of neurons), and maximum in-degree of about 10, indicating that most of the cells are starting to have incoming connectiond from others, but generally not more than ten. By 21 DIV, the growth rate 2 μm/day produces a peak density at in-degree of about 5 (20 % of neurons, same as growth rate 10μm/day at 4 DIV). Growth rate 10 μm/day produces a very flat in-degree distribution, most in-degrees being well over 20 and even beyond 50, indicating that all cells tend to have tens of incoming connections.

With CX3D (figure 5.8, second row), at 4 DIV the in-degree distributions of growth rates 2 μm/day and 22μm/day are very similar to NETMORPH 4 DIV 2 μm/day and 10 μm/day, respectively. This shows that CX3D produces in-degree distributions similar to those of NETMORPH, but the neurite growth rates required to produce them are different. At 21 DIV, the shape of the in-degree distribution of the simulations with a growth rate 2 μm/day has not changed remarkably, showing that neurites grow so slowly that very few connections are formed even by the end of third week of simulated growth. The in-degree distribution produced by growth rate 22 μm/day at 21 DIV has considerably flattened and widened, its peak density

being between 20 and 40 incoming connections (5 % of neurons), and in-degrees of less than 10 being almost nonexistent. This indicates that all of the cells are well connected to others, most having incoming connections from a few tens of cells.

These results indicate that with the proper choice of parameters, NETMORPH and CX3D can produce qualitatively similar results for the in-degree distribution. This requires setting the growth rate of neurites in CX3D slightly higher than in NETMORPH.

Model 2. With NETMORPH Model 2 (figure 5.8, third row), compared to a 100 cell network with the same growth rate, the 1000 cell network produced a similar in-degree distribution. The shape and peak position of the in-degree distribution varied in a similar way in both, starting with sharply downward-sloping distribution witha peak was at in-degree 0 (60 % of neurons) at 4 DIV, and ending up with a more spread out distribution with a peak around 3 incoming connections (20 % of neurons) at 21 DIV. This indicates that also in the bigger network, the slow neurite growth rate prevents cells from forming extensive connectivity in 21 days of simulated time.

5.2.2 Shortest path length

Model 1. The shortest path length distributions vary significantly with simulation time and neuritic elongation rate (Figure 5.9, two upper rows). In the shortest path length analysis histograms where the x axis represents the mean shortest path length, and y axis represents the mean percentage of cells having a particular shortest path length. In the three uppermost rows, the curve colors indicate the basal dendrite growth rate used in the simulation. Growth rates of other neurites scale according to this, apical dendrites having a growth rate two times faster than the basal dendrites, and axons of all neurons 4,5 times faster than the basal dendrites. All dendrites of multipolar neurons grow at the rate of basal dendrites of pyramidal neurons. In the lowest row, the curve colors indicate the attraction parameter values.

With the smaller neurite elongation rates, the shortest path length distribution is a sharply decreasing curve with the peak at zero at 4 DIV. The shortest path zero is not an actual possible shortest path between two cells, but indicates that no path at all was found between a pair of cells. This demonstrates that in the beginning, not that many connections exist in the cultures with low growth rates of neurites. No long-distance connections exist, and connections tend to occur only between immediate neighbors. By 21 DIV the distribution spreads out considerably, and has a very flat shape, indicating that cells even far away from each other could

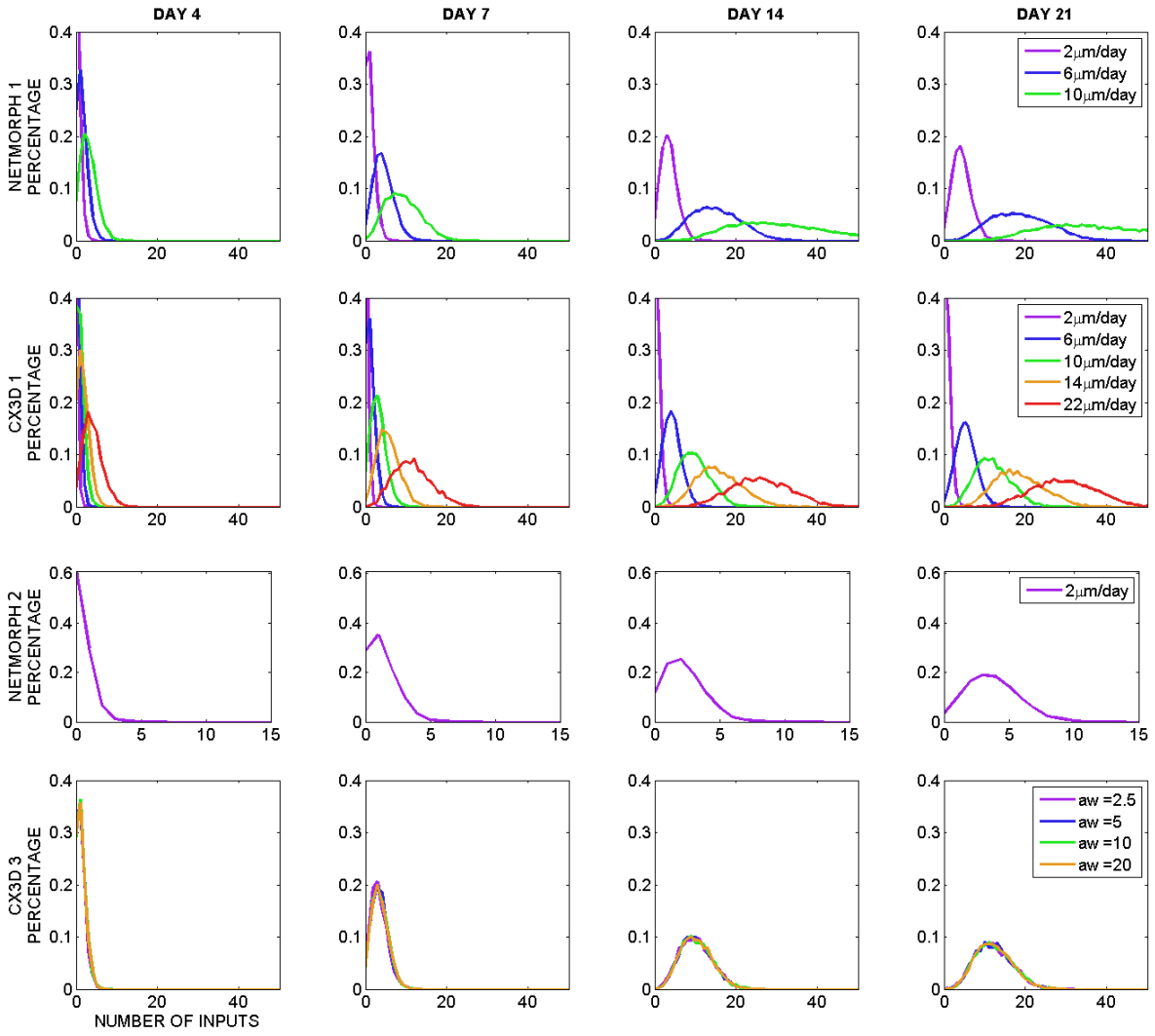

Figure 5.8: Mean in-degree distributions of the simulated neuronal networks. Columns from left to right: 4 DIV, 7 DIV 14 DIV and 21 DIV in simulation time. Rows from top to bottom: NETMORPH1, CX3D1, NETMORPH2, CX3D3. The x axis represents the mean in-degree, and the y axis represents the percentage (as a decimal fraction) of neurons having each in-degree. On the three uppermost rows, different colors represent different growth rates of basal dendrites. Apical dendrites grow at a rate two times faster than the basal dendrites, and axons of all neurons at a rate 4,5 times faster than the basal dendrites. All dendrites of multipolar neurons grow at the rate of basal dendrites of pyramidal neurons. On the lowest row, different colors represent different values of the CX3D attraction parameter.

be connected through several cells between them. With NETMORPH, the basal dendrite growth rate producing this kind of behavior is 2 μm/day, and with CX3D, 6 μm/day. For these cases, at 4 DIV the distribution peak is at shortest path length of 0 (a bit more than 70 % of neurons), and the maximum shortest path is less than 5. At 21 DIV in NETMORPH with a growth rate 2 μm/day distribution has a peak around the shortest path lengths 1-6 (10 % of neurons), and maximum shortest path length is about 15. For networks simulated with CX3D, for basal dendrite growth rate 6 μm/day, the distribution has a peak of mean shortest paths at around 3 (20 % of neurons), and the maximum shortest path length is less than 10. With the basal dendrite growth rate of 2 μm/day, the simulations in CX3D seem to start behaving in a similar way, but the shortest path distribution has not yet obtained a flat shape at 21 DIV.

Conversely, at 4 DIV, the networks with bigger elongation rates have a shortest path length distribution that has a more bell-like shape, and a peak situated the farther from zero the bigger the elongation rate was. This means that the cells have already formed connections to neurons further away through other neurons residing between them. By 21 DIV, the peak of these distributions moves towards zero, and their shape gets sharper. Such behavior indicates that the neurites have grown so long that neurons are capable of connecting many neurons residing far away with their own neurites, thus decreasing the number of "jumps" required to connect any pair of neurons. All other than the before-mentioned growth rates produce this kind of behavior. With NETMORPH and basal dendrite growth rate 10 μm/day at 4 DIV, the peak is around shortest path lengths 1-5 (10 % of neurons), with maximum shortest path of about 15, and at 21 DIV the distribution peak is at shortest path length of 2 (60 % of neurons). With CX3D and growth rate 22 μm/day, at 4 DIV the peak is at shortest path of 3 (20 % of neurons) and maximum shortest path is about 10. At 21 DIV, the peak of this distribution is at shortest path of 2 (about 65 % of neurons), and the maximum shortest path is 3.

Model 2. Compared to the 100 cell network, the 1000 cell network produce similar shortest path length distributions for 4 and 7 DIV, but after that the results are different (see Figure 5.9). At 14 DIV, the peak of the 1000 cell network shortest path length distribution is a bit less than twice as high as the peak of 100 cell network distribution, although their shape is similar. At 21 DIV the distributions are quite different. Whereas the 100 cell network maintains a similar distribution as at 14 DIV, for the 1000 cell network the distribution has spread out considerably, and its peak has moved from 0.2 at shortest path 2 to 0.03 around shortest path 10-20. The results are shown in Figure 5.9, third row from the top.

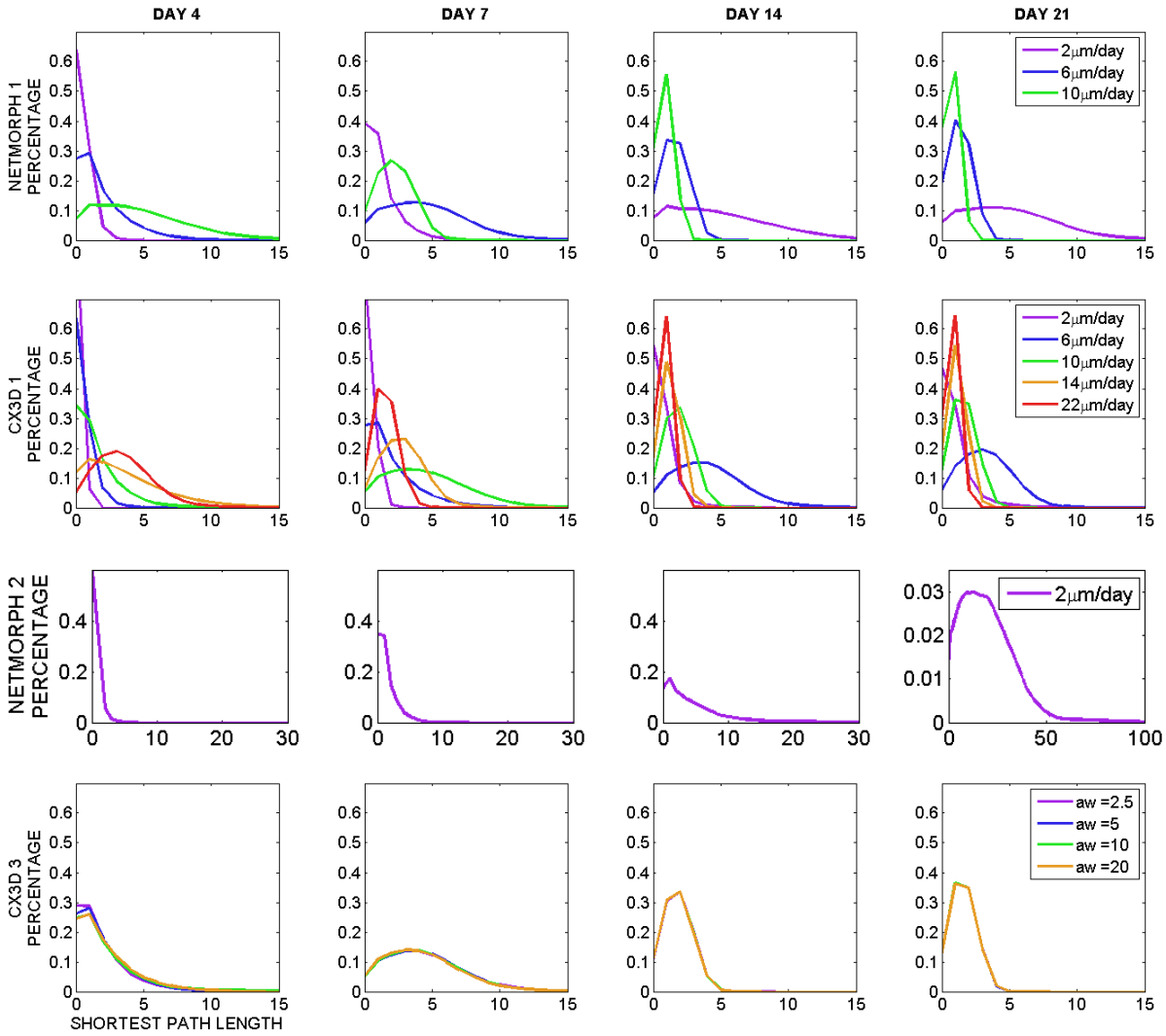

Figure 5.9: Mean shortest path length distributions of the simulated neuronal networks. Columns from left to right: 4 DIV, 7 DIV 14 DIV and 21 DIV in simulation time. Rows from top to bottom: NETMORPH1, CX3D1, NETMORPH2, CX3D3. The x axis represents the mean shortest path length, and the y axis represents the percentage (as a decimal fraction) of pairs of neurons having each shortest path length. On the three uppermost rows, different colors represent different growth rates of basal dendrites. Apical dendrites grow at a rate two times faster than the basal dendrites, and axons of all neurons at a rate 4,5 times faster than the basal dendrites. All dendrites of multipolar neurons grow at the rate of basal dendrites of pyramidal neurons. On the lowest row, different colors represent different values of the CX3D attraction parameter.

5.2.3 Motifs

The motif composition analysis (figure 5.10) shows the percentages of each of the 13 different motifs out of all motifs appearing in the simulated neuronal networks. The x axis represents the different motifs from 1 to 13, and the y axis represents the percentages fo the motifs. In figure 5.10 in the three uppermost rows, the curve colors indicate the basal dendrite growth rate used in the simulation. Growth rates of other neurites scale according to this, apical dendrites having a growth rate two times faster than the basal dendrites, and axons of all neurons 4,5 times faster than the basal dendrites. All dendrites of multipolar neurons grow at the rate of basal dendrites of pyramidal neurons. In the lowest row, the curve colors indicate the attraction parameter values.

Model 1. In both NETMORPH and CX3D, the motifs with smaller connectivity generally dominate in the beginning, and motifs with bi-directional connections are rare. As simulation time passes, the number of motifs with bi-directional connections gets higher. With NETMORPH, this is more pronounced than with CX3D. With NETMORPH, all the simulated growth rates give similar results. Some variation exist in the amounts of least connected motifs and the most connected motifs, smaller growth rates having a bit more of the first mentioned, and larger growth rates the last. With CX3D, in addition to this effect, at 4, 7 and 14 DIV the basal dendrite growth rate 2 μm/day produces clearly less motif number three, and more motif number five than might have been expected when looking at the behavior of the motif analysis of other growth rates. In most cases, certain motifs seem to be more associated with lower growth rates, and some with higher ones. The results are shown in Figure 5.10, two upper rows.

A statistical analysis was performed to determine which of the motifs appeared less and which appeared more in the simulated networks than in random networks with the same average in-degree. The test used was t-test with a confidence level of 0.01. Only networks simulated with Model 1 were studied with the test. The results are shown in figure 5.11. In the tables, the columns indicate different motifs labeled with M1 for motif 1, M2 for motif 2 and so on. The rows are divided in blocks representing each growth rate, and each single row represents the simulation time. The colors indicate how frequently a particular motif is encountered compared to a random network. Dark grey denotes less frequent than in random network and light grey denotes more frequent than in random network. White denotes the same frequency as in random network.

Some trends can be observed in the results. In both NETMORPH and CX3D,

the less connected motifs tend to appear more often, and more connected motifs less often than in a random network. Also with both simulation tools, increasing neurite growth rates and later simulation days tend to make all motifs appear more often than in a random network. Only rarely no statistical difference between the simulated and random networks is not found. The motifs with only two connections between the triplet, namely, motifs 1, 2 and 4, are always represented in larger numbers compared to a random network.

Model 2. The model with a network of 1000 cells produces similar results as the model with 100 cells with the same neurite growth rates (basal dendrite growth rate 2 μm/day). The percentages of the motifs are very similar, but motif 2 is a bit more often present in the 1000 neuron networks than in the 100 neuron networks. The results are shown in Figure 5.10, third row from the top.

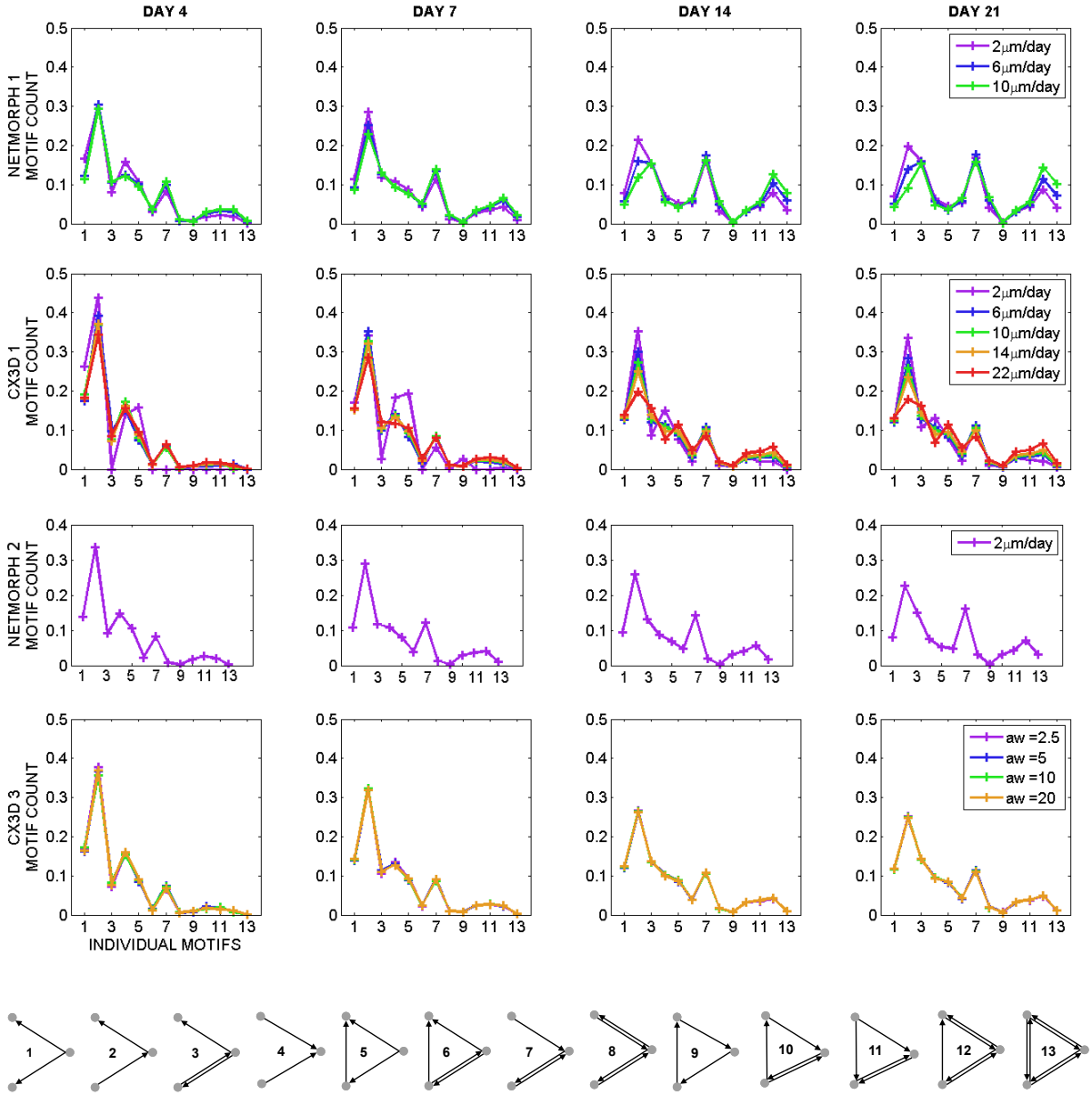

Figure 5.10: Motifs appearing in the simulated neuronal networks. Columns from left to right: 4 DIV, 7 DIV 14 DIV and 21 DIV in simulation time. Rows from top to bottom: NETMORPH1, CX3D1, NETMORPH2, CX3D3. The x axis represents each of the 13 motifs, and the y axis represents the percentage (as a decimal fraction) of each motif out of all motifs appearing in the simulated neuronal networks. On the three uppermost rows, different colors represent different growth rates of basal dendrites. Apical dendrites grow at a rate two times faster than the basal dendrites, and axons of all neurons at a rate 4,5 times faster than the basal dendrites. All dendrites of multipolar neurons grow at the rate of basal dendrites of pyramidal neurons. On the lowest row, different colors represent different values of the CX3D attraction parameter. Below: graph representations of the 13 motifs.

NETMORPH Model 1

	DIV	M1	M2	M3	M4	M5	M6	M7	M8	M9	M10	M11	M12	M13
$2\frac{\mu m}{day}$	7													
	14													
	21													
$6\frac{\mu m}{day}$	7													
	14													
	21													
$10\frac{\mu m}{day}$	7													
	14													
	21													

CX3D Model 1

	DIV	M1	M2	M3	M4	M5	M6	M7	M8	M9	M10	M11	M12	M13
$2\frac{\mu m}{day}$	7													
	14													
	21													
$6\frac{\mu m}{day}$	7													
	14													
	21													
$10\frac{\mu m}{day}$	7													
	14													
	21													
$14\frac{\mu m}{day}$	7													
	14													
	21													
$22\frac{\mu m}{day}$	7													
	14													
	21													

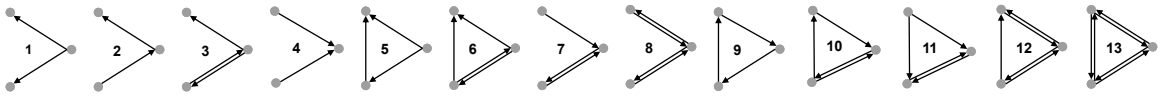

Figure 5.11: Tables of statistical differences between the simulated networks and random networks. Table above: NETMORPH Model 1. Table below: CX3D Model 1. Columns indicate the 13 motifs (M1-M13), and rows indicate the growth rate and simulation day. Dark grey: The motif in question was present in statistically significant lower quantity than in a corresponding random network. Light grey: The motif in question was present in statistically significant higher quantity than in a corresponding random network. White: No statistical difference in occurrence of the motif between simulated and random network. Below: graph representation of the 13 motifs.

6 Discussion

The aim of this M.Sc. thesis is to compare CX3D and NETMORPH, two recently published neuronal network growth simulation tools. Three models were built and simulated to facilitate comparison. In this section the models, results, and simulation tools are discussed. Comparison of CX3D and NETMORPH is mainly under section 6.3.2, but is discussed in most of the following sections.

The work presented here is the first existing comparison between the two simulation tools, CX3D and NETMORPH. These are the first simulation tools for simulating the morphological development of neuronal networks. Other neuronal simulation tools such as NEST (Gewaltig & Diesmann, 2007), NEURON (Carnevale & Hines, 2006) and GENESIS (Bower et al., 2003) exist, but they are incapable of simulating growth of neurons.

6.1 User experiences

The basic use of both tested simulation tools requires some knowledge in software engineering, scientific computing and programming. Both tools are provided with a comprehensive manual and example pieces of code that can be tested. Especially CX3D provides several colorful examples which, from a biologist's point of view, illustrate different kinds of possibilites with the tool. Although a biologist might be able to run simulations by making simple changes in the provided example code, larger changes require deeper understanding of the tool and code as a whole. Interpreting the results also requires knowledge in computer science. Therefore, the use of these tools requires a biologist to have a scientist trained in computer science by their side. An interface specifically designed for biologists would facilitate independent work of biologists with these tools.

Implementing the same model in both simulation tools was not stragihtforward, because the differing intrinsic properties of the tools made it impossible to build the models exactly equally. Knowing the difference in the view point of the tools, this was not completely unexpected. Understanding the consequences of different choices of modeling strategies also requires some insight into modeling.

The graphical user interface of CX3D makes it easy to follow the development of the simulated network of neurons, and facilitates the usability for biologists. However, when running a large number of simulations on a server, the graphical user interface is not needed, and a simple way of turning it off is required. In this sense NETMORPH is more straightforward to run on a server.

6.2 The built models

6.2.1 Summary of model properties

The built model of neuronal growth contains a description of two kinds of cells: pyramidal and multipolar. Pyramidal cells have 2-5 basal dendrites, one apical dendrite and one axon. Multipolar cells have 2-5 basal dendrites and one axon. The distinction between pyramidal and multipolar in the model is purely morphological, as bioelectrical activity is not included in the model. The models are constructed based on earlier work by van Pelt et al. In Model 1 simulations, the neurite growth rate parameters were varied to study the effects of growth rate of neurites to the connectivity of the formed network. With Model 2, a ten times larger network was simulated to study the effects of network size to the properties of the formed network. In Model 3, the attraction parameter of CX3D was varied to study if it is possible to use the parameter as a simplified model of molecular guidance cues.

When discussing the different growth rates of neurites, the growth rates used in the simulation are expressed through declaring the basal dendrite growth rate of pyramidal dendrites in the simulations. Growth rates of other neurites always scale relative to this. For pyramidal neurons, the apical dendrite growth rate is two times that of the basal dendrite growth rate, and for multipolar neurons, the growth rate of all dendrites is the same as the basal dendrite growth rate of pyramidal neurons. Axons of neurons grow at a rate 4,5 times higher than the basal dendrite growth rate of pyramidal neurons.

Because the possibility to simulate molecular diffusion exists only in CX3D but not in NETMORPH, guidance cues were not simulated through molecular diffusion. Choosing to leave this out of the model also simplifies it, which is desirable in the beginning stages of building a new model. Cell death was also left out of the simulations because only CX3D would have been able to include it. Network size was 100 in Models 1 and 3, and 1000 in Model 2 to ensure that both simulation tools would be able to simulate the models efficiently.

6.2.2 Limitations and future improvement

In the models used in this study, the axons and dendrites start their growth simulataneously in the models. To compensate for the experimentally observed initial growth of axons, during which dendrites do not grow, the simulations were initialized with axons which already have an initial length. Because the simulations do not start from zero length of all neurites, it could be argued that the initial conditions do not correspond to 0 DIV, that is, the time of plating of the neurons. The simulated days are not far from the "realistic" days in culture, because this initial axonal growth without any dendritic growth only lasts for a day (de Lima et al., 1997). Thus one or two days might be added to the age of the simulated cultures to find the day in culture that it realistically represents.

The apical dendrites of pyramidal neurons in the models are not based on exact reconstructions of a real apical dendrites *in vitro*. The existing morphological data is from *in vivo* apical dendrites which have a long stem with so called oblique branches along it, and a tuft in the distal end. Neurons in the models built for this work have simplified apical dendrites modeled according to visual inspection of images of cultured neurons in the literature. The apical dendrites of cultured neurons lack many of the characteristics of the *in vivo* apical dendrites, for example the tuft and oblique branches. In the models, apical dendrites have the same morphology as basal dendrites, and a growth rate twice that of the basal dendrites. It would bring more realistic features to the morphology neurons to reconstruct these after experimentally obtained statistical data about apical dendrites *in vitro* (Donohue & Ascoli, 2010).

In NETMORPH the simulations are truly two-dimensional, whereas in CX3D, the third dimension is necessary due to the simulator's space discretization method. This means that unlike in NETMORPH, in CX3D the neurites grow in all three dimensions. The simulation space is a flat disc with 10 μm thickness, correspondinc to the diameter of a single neuron to ensure that the neurons cannot be placed on top of another. However, the thickness allows dendrites to grow also in the z dimension, not only planar as in NETMORPH. This affects neuronal growth and produces some unrealistic morphologies.

Because the models used in this study are simplified in order to facilitate easy comparison, they do not excactly represent the situation in a real neuronal culture. One critical example is the slowing of growth. In cell cultures, growth slows down as the plate becomes more crowded and neurites become longer, making it more difficult to transport the structural proteins needed for growth to the tip of the neurite. In

the simulated models, slowing of growth due to the increase in the number of neurite tips, might not be fast enough. In CX3D, it is possible to simulate cell death, which might bring a more realistic aspect into the simulated model. It might be interesting to give some conditions for survival of neurons, *e.g.* a sufficient number of contacts to other neurons by a certain simulation day, if a correlation between connectivity and survival is found in cell culture experiments (Aćimović et al., 2011).

6.3 Simulated neuronal features and networks

6.3.1 General observations

The Sholl analysis of axons shows that in networks simulated with both simulation tools, the mass of axonal branches is located in the middle parts along the length of axonal field. Both tools produce a similar distribution of axonal length, but in NETMORPH, the number of axons crossing the Sholl radius circles is considerably higher. This shows that axons in NETMORPH branch more than in CX3D.

In the networks simulated with both simulators, the overall shape of dendritic Sholl analysis histograms is also similar: a "bump" followed by a tail for pyramidal cells, and a mere "bump" for multipolar cells (figures 5.2 and 5.3). The bump represents the basal dendrites of the pyramidal cells and all the dendrites of multipolar cells, which are more numerous than the apical dendrites, and also elongate slower. The longer apical dendrites make up the tail of the Sholl analysis histogram for dendrites.

Higher growth rates produce higher numbers of synapses, because the longer the neurites become, the bigger chance they have of encountering a partner for synapse formation. This is also the reason the number of synapses grows with passing simulation time with any growth rate of neurites.

The experimentally defined synapse count and the count obtained from the simulated neuronal networks are calculated differently, and this is taken into account when analyzing the results. It is evident from the synapse counts that the number of synapses per neuron grows exponentially with time. The experimentally observed numbers of synapses, however, become stable after 14 DIV (Ichikawa et al., 1993). It is clear that in a cell culture the number of synapses cannot grow uncontrollably. There are two factors limiting the number of synapses in culture: apoptosis of cells (Ichikawa et al., 1993) and activity-dependent removal of synapses (Butz et al., 2009; Tetzlaff et al., 2010). These both contribute to loss of excessive synapses, and are

both mechanisms not present in the simulated models. Including these mechanisms in the models would be an interesting continuation to this work.

6.3.2 Model 1 - Effects of growth rate and comparison of the tools

The most notable result when comparing NETMORPH and CX3D is the difference in the morphology these simulation tools produce with the same model (Model 1). It is especially notable that NETMORPH produces dendrites that are longer and branch more, because it is textbook knowledge that the dendritic field of a neuron determines the possible extent of its connectivity to other neurons (Purves et al., 2008). This is the result explaining most of the observed differences in all the other results, also part of the difference in numbers of synapses per neuron. In NETMORPH, most of the larger amount of synapses per neuron, compared to CX3D, represents connections to a bigger amount of other neurons, as seen in the in-degree distributions (figure 5.8). NETMORPH produces a very large amount of synapses with all growth rates from the beginning of the simulation, and ends up producing networks with several times more synapses compared to what has been experimentally observed. Part of the differences in synapse counts can also be explained by production of more synapses between the same pair of neurons, which does not show in the in-degree distribution.

The higher connectivity in the neuronal networks simulated with NETMORPH can be seen from the tendency of the NETMORPH in-degree distributions to resemble the in-degree distributions obtained with higher growth rates in CX3D. For example, Model 1 simulated with NETMORPH with a basal dendrite growth rate of 2 μm/day produces a similar in-degree distribution as CX3D model with a basal dendrite growth rate of 6 μm/day (figure 5.8). Likewise, NETMORPH Model 1 with a basal dendrite growth rate of 6 μm/day produces a distribution similar to CX3D Model 1 with a basal dendrite growth rate of 14 μm/day. In the mean shortest path distributions, NETMORPH Model 1 with a basal dendrite growth rate of 6 μm/day and CX3D Model 1 with a basal dendrite growth rate of 10 μm/day resemble one another (figure 5.9). In the motif composition analysis (figure 5.10), higher connectivity likely also explains the tendency of NETMORPH to produce higher percentages of the more connected motifs, and consequently the lower percentages of the less connected motifs.

CX3D generally shows a better fit with the experimentally observed synapse counts. The basal dendrite growth rate 14 μm/day produces results closest to the experimen-

tally observed ones up until 14 DIV . After that, however, it also produces too many synapses, and by 21 DIV it has produced more than two-fold number of synapses compared to experimental observations. At 21 DIV the basal dendrite growth rate 10 μm/day produces results closest to the experimental ones. With NETMORPH, until 14 DIV the basal dendrite growth rate 6 μm/day produces results comparable to the experimentally observed ones. After that, the obtained simulation results deviate from the experimentally observed ones. This happens because both models produce an excessive number of synapses, and because the synapse removing mechanisms, discussed in section 6.3.1, are missing. In the new version of NETMORPH, there is an improved synapse model (van Pelt et al., 2010), which solves the excessive synapse formation for three-dimensional models. The new synapse model was released after this work was completed.

6.3.3 Model 2 - Effects of network size

A larger network was simulated to test the effects of network size on the properties of the produced network. The larger network size results in more synapses per neuron, probably because the neurons have more targets to form synapses with. Mean in-degree stays about the same. Mean shortest path length starts out the same, but ends up having much higher values in the end, because very long-distance connections form because distant areas of the culture become connected through neurons residing between them as simulation time passes. Motif composition stays about the same, because motifs tend to occur between close neighbors more often than between distant neighbors. Thus when cell density stays the same, the average number of close neighbors of each cell stays the same. The small increase in the percentage of the least connected motifs could be explained by the fact that while a neuron may well connect with a very distant partner when its neurites have grown to a considerable length, it is much more unlikely that bi-directional connections will form between the distant pair of neurons, or between this pair and the third neuron of the triplet. Thus in a culture with long-distance connections, one would expect to get a bigger percentage of less connected triplets.

Although the size of the neuronal network was ten times larger in Model 2 than in Model 1, it may still be too small to produce phenomena that would occur only in truly large networks. The current version of NETMORPH requires too much memory space for storing the results, and therefore the maximal size of networks that can be simulated is around 1000 neurons. The new version of NETMORPH, with its improved synapse formation model (van Pelt et al., 2010), is less memory

demanding and will provide a possibility to simulate bigger networks. Therefore, it can be used for additional testing of the influence of network size on the examined graph theoretical measures.

6.3.4 Model 3 - Effects of attraction parameter variation

The third model was simulated in order to study the effects of varying the attraction parameter controlling an attractive force between axons and cell bodies. Varying the attraction parameter in CX3D does not have any effect on the development of the simulated networks. One possible reason for this is that the radius of effectivenes of the attractive force around the soma is not large enough to cause any considerable deviation of axons from their former paths. Apparently, an axon that has already come within the range of the attraction, is in any case close enough to likely form synapses with the nearby dendrites. In this model, synapses between neuronal cell bodies and axons are not created, and thus attracting an axon to grow close to a soma does not promote synapse formation directly, but possibly indirectly by bringing the axon closer to dendrites. The other possibility is that the attraction parameter was not set strong enough to have any effect. Further testing is needed to find out the suitability of this parameter for simplified modeling of attractive guidance cues. The exact way to model guidance cues would be to model their molecular diffusion and detection by axons, which is possible in CX3D but not in NETMORPH.

6.3.5 Achievements of the model

In general, the synapse counts of the simulated neuronal networks are within the range of experimentally observed values with the tested biologically realistic growth rates. This indicates that the models are successful in describing neuronal growth in a simplified way. Unfortunately the other computed measurements of neuronal morphology and network characteristics are difficult to obtain in experimental studies of cell cultures after the first days. This makes assessing those results' similarity to experimental data impossible at the moment. Hopefully with the development of culturing techniques, possibly combined with automated imaging, also these results can be evaluated. This would facilitate developing the models further.

6.3.6 Zig-zag anomalies of neurites in CX3D

The observed zig-zags in neurites (section 5.1.2) are a problem specific to the built CX3D models, and they appear probably due to the nature of the physics simulator behind the movement of physical objects in the simulations. Limiting the simulation of a neuronal culture in a very flat space resembling the culture dish causes the problems. The zig-zag seems to form an about 10 μm wide pattern - the width that was used to define the z dimension, that is, the thickness of the "plate" in the simulations. This thickness was chosen so that the neuronal cell bodies, which are also 10 μm in diameter, will not grow on top of each other, because such a phenomenon is not observed in healthy neuronal cell cultures. The physics simulator of CX3D prevents objects from perforating one another by placing a repulsive force between two objects if they have ended up occupying the same physical space after a simulation step. It also keeps objects in the simulation space by creating a force pushing an object back inside the space boundaries if it has ended up outside of the simulation space. It is likely that the zig-zags are formed when a growth direction towards the z dimension (for example, the "top" of the plate) has been chosen for a neurite, causing it to bounce back when it ends up outside of the simulation space as a result of this choice of direction. The bounce might direct it towards the the other boundary of the z dimension (now, the "bottom" of the plate), and create a recurring chain of events where the growing neurite ends up bouncing back and forth between the z dimension boundaries. This kind of behavior could cause the observed 10 μm zig-zag pattern.

This reveals an essential difference between real-life conditions and simulation conditions in CX3D. Beacuse the cell bodies and neurites in the simulation are not anchored in the simulation space by any force such as friction, they are free to move every time a force is exerted on them. In the environment of a real cell culture, the neurons are always attached to the plate substrate and cannot be easily pushed to move. Also, in a cell culture, the only support for the neurons is the flat bottom of the culture dish, and as a result they will grow flat on the dish floor. Because CX3D was primarily intended for simulating 3D tissue structures, it does not take into account some special conditions on a culture dish, and might require some modifications to be better suited for "2.5D" simulations (as the authors of CX3D call it) intended for studying neuronal growth on a culture plate. This problem could be solved by limiting the growth of neurites in the z dimension, for example by implementing an additional force which keeps the neurites in the bottom of the dish.

6.3.7 Applicability of the simulation tools

CX3D and NETMORPH are inherently very different in nature. Where in CX3D it is possible to include high levels of detail, modeling in NETMORPH is done in a more phenomenological way. This suggests that CX3D might be best applied to study of small scale phenomena including, for example, molecular diffusion of guidance cues in small neuronal networks, or other phenomena which are best studied when there is no need to make an educated guess about the approximate effect of small-scale phenomena. NETMORPH, on the other hand, is powerful in its capability to simulate also larger networks, which are interesting for the study of phenomena occurring in the living brain. NETMORPH is therefore well suitable for studying the formation of large networks, and graph theoretical analysis of large networks. These two simulation tools could possily support each other in the study of neuronal networks. The overall effects of small-scale events could be studied through simulating models in CX3D, and the obtained insight could be transferred to the NETMORPH model by fine-tuning the equations, to be used in simulating large neuronal networks.

6.4 Requirements computational modeling sets on experimental work

For building a model of a biological process, based on experimental data, two sets of data are needed: one for constructing the model, and one for validating it. For constructing the model, neurite elongation and branching has to be parametrized. For validating the model, data about synapse fotmation at different developmental days needs to be collected. The morphological data found in the literature is mainly *in vivo* data (collection of such data can be found in www.neuromorpho.org). However, *in vitro* data for modeling is also needed, since the cell culture setup is a very feasible way of studying formation and functioning of neuronal networks. On a plate, the culture is easily imaged with microscopy techniques, and its bioelectrical activity can be monitored with the microelectrode array (MEA) technique. The conditions of a cell culture can be monitored and modified to study different kinds of phenomena. Cell cultures are also free of many ethical concerns. The problems with the available *in vitro* data are in the consistency and optimization of culturing conditions (Teppola, 2008).

It has been observed that when culturing neurons, the main physiological phenomena

of growth and bioelectrical activity persist in the culture independent of exact growth conditions (Marom & Shahaf, 2002). However, this does not guarantee that any kind od cell culture data is usable when building models of neuronal network behavior. In order to analyze the dynamics of growth, the conditions leading to the final outcome should be recorded in high detail. In order to produce a data set that is consistent, the culturing conditions should be stabile and carefully monitored.

Drifting of culturing conditions (such as hyperosmolality, discussed by Potter & DeMarse, 2001) might affect the behavior of neurons in an unknown way. Observing neuronal network formation and maturation requires maintenance of the cell cultures for up to a month or more. Thus the challenges of long-term culturing become an essential question to be taken into account. Since culturing conditions influence the growth of neurons and formation of networks (*e.g.* Ichikawa et al., 1993; de Lima et al., 1997), it is very important to carefully keep the culturing conditions stable and record them well, to produce comparable data. Optimizing long-term culture conditions is not very easy, but some techniques have been developed to keep neuronal cultures alive, and presumably healthy, for even more than a year (Potter & DeMarse, 2001). However, these have not been very widely in use, and a wealth of existing data dates back to the time when the more accurate culturing techniques were not yet in use.

Some problems of keeping neurons in an environment as native as possible arise from a clash between optimal conditions for neurons and optimal conditions for studying them. Neurons do not grow healthy in low cell densities in which they have few neighbors to contact. Hence, to obtain healthy behavior in the culture, they should be grown in a sufficiently dense neuronal neighborhood. However, detection of neuronal features in dense cultures is difficult from the beginning, and becomes impossible after the first week in culture because of the neurites covering the plate in an unsortable manner.

The presence of glial cells is one growth effecting factor that varies with the used protocol (see table 2.1). Because the glia provide important metabolism supporting neuronal functions, and they are a natural effector in the neurons' natural tissue environment, their presence, or the lack of it, influences neuronal growth. It has been shown that with an astroglial feeder layer, neurons in the culture polarize faster and are able to grow in smaller plating densities (de Lima et al., 1997). This assists the long-term survival of neurons. If the glia are removed from direct connection with the neurons, they are removed by using a mitotic inhibitor, usually cytosine arabinoside. This chemical is also toxic to neurons, although less so than for the glia, and its usage affects the growth of neurons at the time of use. Removing the glia

has also been shown to induce the formation of a small subpopulation of GABAergic neurons in the culture, which resembles basket cells of the brain (de Lima & Voigt, 1999). The glia might thus have yet unknown effects on the growth of neurons.

Variation in the maintenance of long-term cultures is probably a major source of variation in the experimental results, and often cannot be clearly pointed out based of the literature. The exact effect of this variance on modeling can only be guessed, but should be taken into account as a possible source of error.

The ideal set of data for modeling would consist of a large number of repetitions for each experimental setup. The number of repeated experiments should be high enough to produce statistical data for both model tuning and model validation. Conditions on the culture plate should be monitored tightly, kept as stable as possible and recorded at all times. The experimental protocols should be well documented and published to allow exact reproduction of the experiments. An on-line database designed for storing data from such experiments would be an ideal way to share the data with the community.

The International Neuroscience Coordination Facility (INCF, www.incf.org) has an initiative towards this goal. It has a program to develop standards for sharing neuroscience data and tools to facilitate recording, sharing and reporting of metadata. The outcomes of this program are likely to help considerably with the current issues with using experimental data in modeling.

6.5 Contribution of the work

The aim of this work was to find out what experimental data about neuronal morphology in cell cultures exists in the literature, and to build a model of morphological development of neurons in a cell culture based on that data and existing models. The motivation for this aim was to facilitate combining two experimental setups, the flexible biological *in vitro* set up and the computational *in silico* research method.

This work contributes to the study of biology and modeling of biology. For biologists, it brings insights into how the same biological process might be modeled in two different ways, and what are the limitations when mathematically modeling processes that in nature have details on the molecular level. This work also points out the need for constructing experiments that fulfill the needs of modelers.

For computational scientist, the thesis shows a biologist's point of view on using simulation tools. The thesis also compares two newly published simulation tools and

describes the results they produce when modeling neuronal growth, their strengths and their differences. This work shows that the tools are capable of producing qualitatively similar results with the correct choice of model parameters.

The results of this work can be used when choosing a simulation tool to be used in *in silico* experiments, or when designing experimental protocols for obtaining biological data for modeling. This work also serves as a basis for further development of the model built for this work.

7 Conclusions

The purpose of this study was to evaluate and compare two neuronal growth simulation tools, CX3D and NETMORPH. This was done through attempting to implement the same model of neuronal growth in both, and comparing the obtained results to each other, and also to experimental data found in the literature.

Implementing the same model in both simulation tools was not straightforward, and it was not possible to make the models exactly equivalent. In addition, morphological data from neuronal cell cultures reported in the literature is scarse and not as well documented as one would hope, and this sets limitations on the biological accuracy of the models and the chosen set of parameters.

Although the tools' intrinsic properties prohibited testing some choices of parameters because of heavy simulations, in general, both of these tools performed as desired. Due to the different nature of the simulators, simulating the same implemented model yielded differences in some of the results. Nevertheless, the aquired results are in the range of biologically meaningful values. With a more detailed study of the tools and parameter space of the simulations, a more realistic representation of development of morphology in neuronal cell cultures could be achieved.

Because these tools are inherently different in nature, they have differing applications. NETMORPH would be best suited for modeling the formation of large neuronal networks, and a following graph theoretical analysis of the simulated networks. CX3D, on the other hand, would be an interesting tool for testing the effects of molecular signals in the formation of smaller neuronal networks.

These new simulation tools are valuable additions to theoretical and experimental studies of cultured neuronal networks. Further development of both tools will enhance their usability. In addition to tool development, suitable datasets should be collected to facilitate creation and fine-tuning of accurate models of neuronal network growth *in vitro*.

8 References

Aćimović J, Mäki-Marttunen T, Havela R, Teppola H, Linne ML. Modeling of Neuronal Growth *In Vitro*: Comparison of Simulation Tools NETMORPH and CX3D. EURASIP Journal on Bioinformatics and Systems Biology , 2011;2011:616382.

Aeschlimann M. Modeling Neural Development. Ph.D. thesis, L'Université de Lausanne, 2000.

Ascoli GA, Krichmar JL, Scorcioni R, Nasuto SJ, Senft SL. Computer generation and quantitative morphometric analysis of virtual neurons. Anat Embryol (Berl) , 2001;204:283–301.

Bekkers JM, Häusser M. Targeted dendrotomy reveals active and passive contributions of the dendritic tree to synaptic integration and neuronal output. Proc Natl Acad Sci U S A , 2007;104:11447–11452.

Bernard A, Sorensen SA, Lein ES. Shifting the paradigm: new approaches for characterizing and classifying neurons. Curr Opin Neurobiol , 2009;19:530–536.

Bower JM, Beeman D, Hucka M. chap. The GENESIS Simulation System, pp. 475–478. MIT Press, second ed., 2003;.

Braitenberg V, Schz A. Cortex: Statistics and Geometry of Neuronal Connectivity. Springer, Berlin, Germany, 1998. ISBN: 3-540-63816-4.

Butz M, Wörgötter F, van Ooyen A. Activity-dependent structural plasticity. Brain Res Rev , 2009;60:287–305.

Carnevale N, Hines M. The NEURON Book. Cambridge University Press, 2006.

Clowry G, Molnár Z, Rakic P. Renewed focus on the developing human neocortex. J Anat , 2010;217:276–288.

Cuntz H, Forstner F, Borst A, Häusser M. One rule to grow them all: a general theory of neuronal branching and its practical application. PLoS Comput Biol , 2010;6.

DeFelipe J, Alonso-Nanclares L, Arellano JI. Microstructure of the neocortex: Comparative aspects. Journal of Neurocytology , 2002;31:299–316.

Donohue DE, Ascoli GA. Automated reconstruction of neuronal morphology: An overview. Brain Res Rev , 2010;.

van Elburg RA, van Ooyen A. Impact of dendritic size and dendritic topology on burst firing in pyramidal cells. PLoS computational biology , 2010;6.

Gewaltig M, Diesmann M. NEST. Scholarpedia , 2007;4:1430.

Gilmore EC, Herrup K. Cortical development: layers of complexity. Curr Biol , 1997;7:231–234.

Graham BP, van Ooyen A. Mathematical modelling and numerical simulation of the morphological development of neurons. BMC Neurosci , 2006;7 Suppl 1.

Harris KM. Structure, development, and plasticity of dendritic spines. Curr Opin Neurobiol , 1999;9:343–348.

Hering H, Sheng M. Dendritic spines: structure, dynamics and regulation. Nat Rev Neurosci , 2001;2:880–888.

Higginbotham H, Yokota Y, Anton ES. Strategies for Analyzing Neuronal Progenitor Development and Neuronal Migration in the Developing Cerebral Cortex. Cereb Cortex , 2010;.

Ichikawa M, Muramoto K, Kobayashi K, Kawahara M, Kuroda Y. Formation and maturation of synapses in primary cultures of rat cerebral cortical cells: an electron microscopic study. Neurosci Res , 1993;16:95–103.

Jan YN, Jan LY. The control of dendrite development. Neuron , 2003;40:229–242.

Jimbo Y, Tateno T, Robinson HP. Simultaneous induction of pathway-specific potentiation and depression in networks of cortical neurons. Biophys J , 1999;76:670–678.

Kato-Negishi M, Muramoto K, Kawahara M, Kuroda Y, Ichikawa M. Developmental changes of GABAergic synapses formed between primary cultured cortical neurons. Brain Res Dev Brain Res , 2004;152:99–108.

Kiddie G, McLean D, Van Ooyen A, Graham B. Biologically plausible models of neurite outgrowth. Prog Brain Res , 2005;147:67–80.

Koene R, Postma F, de Ridder S, Hoedemaker S, van Pelt A Jand van Ooyen. NETMORPH Manual - Version March 5 , 2009a;.

Koene RA, Tijms B, van Hees P, Postma F, de Ridder A, Ramakers GJ, van Pelt J, van Ooyen A. NETMORPH: a framework for the stochastic generation of large scale neuronal networks with realistic neuron morphologies. Neuroinformatics , 2009b; 7:195–210.

Kriegstein AR, Dichter MA. Morphological classification of rat cortical neurons in cell culture. J Neurosci , 1983;3:1634–1647.

Lesuisse C, Martin LJ. Long-term culture of mouse cortical neurons as a model for neuronal development, aging, and death. J Neurobiol , 2002;51:9–23.

de Lima AD, Merten MD, Voigt T. Neuritic differentiation and synaptogenesis in serum-free neuronal cultures of the rat cerebral cortex. J Comp Neurol , 1997; 382:230–246.

de Lima AD, Voigt T. Identification of two distinct populations of gamma-aminobutyric acidergic neurons in cultures of the rat cerebral cortex. J Comp Neurol , 1997;388:526–540.

de Lima AD, Voigt T. Astroglia inhibit the proliferation of neocortical cells and prevent the generation of small GABAergic neurons in vitro. Eur J Neurosci , 1999; 11:3845–3856.

Mäki-Marttunen T, Havela R, Aćimović J, Teppola H, Ruohonen K, Linne ML. Modeling Growth in Neuronal Cell Cultures: Network Properties in Different Phases of Growth Studied Using Two Growth Simulators. Seventh International Workshop on Computational Systems Biology, WCSB 2010, June 16-18, 2010, Luxembourg , 2010;.

Manninen T, Hituri K, Kotaleski JH, Blackwell KT, Linne ML. Postsynaptic signal transduction models for long-term potentiation and depression. Front Comput Neurosci , 2010;4:152–152.

Marom S, Shahaf G. Development, learning and memory in large random networks of cortical neurons: lessons beyond anatomy. Q Rev Biophys , 2002;35:63–87.

Mason C. The development of developmental neuroscience. J Neurosci , 2009; 29:12735–12747.

Milo R, Shen-Orr S, Itzkovitz S, Kashtan N, Chklovskii D, Alon U. Network motifs: simple building blocks of complex networks. Science , 2002;298:824–827.

Nakanishi K, Kukita F. Functional synapses in synchronized bursting of neocortical neurons in culture. Brain Res , 1998;795:137–146.

Newman ME. The structure and function of complex networks. SIAM Review , 2003;45:167–256.

van Pelt J, Carnell A, de Ridder S, Mansvelder HD, van Ooyen A. An algorithm for finding candidate synaptic sites in computer generated networks of neurons with realistic morphologies. Front Comput Neurosci , 2010;4:148–148.

van Pelt J, van Ooyen A, Uylings HB. The need for integrating neuronal morphology databases and computational environments in exploring neuronal structure and function. Anat Embryol (Berl) , 2001;204:255–265.

van Pelt J, Uylings H. Natural variability in the geometry of dendritic branching patterns. In: Reeke G, Poznanski K, Rosenberg S JR (eds.), Modeling in the Neurosciences - From Biological systems to Neuromimetic Robots, pp. 89–115. Taylor & Francis, Boca Raton, Florida, USA, 2005;.

van Pelt J, Uylings H. Modeling Neuronal Growth and Shape. In: Laublicher MD, Mller GB (eds.), Modeling Biology Structures, Behaviors, Evolution, pp. 195–215. The MIT Press, Cambridge, Massachusetts, 2007;.

van Pelt J, Uylings HB. Branching rates and growth functions in the outgrowth of dendritic branching patterns. Network , 2002;13:261–281.

van den Pol AN, Obrietan K, Belousov AB, Yang Y, Heller HC. Early synaptogenesis in vitro: role of axon target distance. J Comp Neurol , 1998;399:541–560.

Potter SM, DeMarse TB. A new approach to neural cell culture for long-term studies. J Neurosci Methods , 2001;110:17–24.

Purves D, Augustine G, Fitzpatrick D, Hall W, LaMantia AS, McNamara J, White L (eds.). Neuroscience. Sinauer Associates, Inc., Sunderland, Massachusetts, USA, 4th ed., 2008.

Rakic P. Neurogenesis in adult primates. Prog Brain Res , 2002;138:3–14.

Rash BG, Grove EA. Area and layer patterning in the developing cerebral cortex. Curr Opin Neurobiol , 2006;16:25–34.

Saarinen A, Linne ML, Yli-Harja O. Stochastic differential equation model for cerebellar granule cell excitability. PLoS Comput Biol , 2008;4.

Segev I. What do dendrites and their synapses tell the neuron? J Neurophysiol , 2006;95:1295–1297.

Sejnowski TJ, Koch C, Churchland PS. Computational neuroscience. Science , 1988; 241:1299–1306.

Sporns O, Tononi G, Kötter R. The Human Connectome: A Structural Description of the Human Brain. PLoS Comput Biol , 2005;1:e42+.

Stepanyants A, Chklovskii D. Neurogeometry and potential synaptic connectivity. Trends in Neurosciences , 2005;28:387–394.

Teppola H. Ihmisen SH-SY5Y-neuroblastoomasolulinjan käyttöönotto ja erilaistaminen sähköfysiologisia monielektrodimittauksia varten. Master's thesis, University of Tampere, 2008.

Tetzlaff C, Okujeni S, Egert U, Wörgötter F, Butz M. Self-Organized Criticality in Developing Neuronal Networks. PLoS Comput Biol , 2010;6:e1001013+.

Uylings HB, van Pelt J. Measures for quantifying dendritic arborizations. Network , 2002;13:397–414.

Wagenaar DA, Pine J, Potter SM. An extremely rich repertoire of bursting patterns during the development of cortical cultures. BMC Neurosci , 2006;7:11–11.

White JA, Rubinstein JT, Kay AR. Channel noise in neurons. Trends Neurosci , 2000;23:131–137.

Zubler F. CX3D short tutorial - Version 0.5 , 2009;.

Zubler F, Douglas R. A framework for modeling the growth and development of neurons and networks. Front Comput Neurosci , 2009;3:25–25.